



Original article

Design and structure activity relationship of tumor-homing histone deacetylase inhibitors conjugated to folic and pteric acids



Quaovi H. Sodji^a, James R. Kornacki^{d, e}, John F. McDonald^{b, c}, Milan Mrksich^{d, e, **}, Adegboyega K. Oyelere^{a, c, *}

^a School of Chemistry and Biochemistry, Georgia Institute of Technology, Atlanta, GA 30332-0400, USA

^b School of Biology, Georgia Institute of Technology, Atlanta, GA 30332-0400, USA

^c Parker H. Petit Institute for Bioengineering and Bioscience, Georgia Institute of Technology, Atlanta, GA 30332-0400, USA

^d Department of Chemistry, Northwestern University, 2145 Sheridan Road, Evanston, IL 60208-3113, USA

^e Department of Biomedical Engineering, Northwestern University, 2145 Sheridan Road, Evanston, IL 60208-3113, USA

ARTICLE INFO

Article history:

Received 21 August 2014

Received in revised form

3 April 2015

Accepted 4 April 2015

Available online 8 April 2015

Keywords:

Targeted delivery

Histone deacetylase

Folate

Pteric acid

Hydroxamic acid

Tubastatin A

ABSTRACT

Histone deacetylase (HDAC) inhibition has recently emerged as a novel therapeutic approach for the treatment of various pathological conditions including cancer. Currently, two HDAC inhibitors (HDACi) – Vorinostat and Romidepsin – have been approved for the treatment of cutaneous T-cell lymphoma. However, HDACi remain ineffective against solid tumors and are associated with adverse events including cardiotoxicity. Targeted delivery may enhance the therapeutic indices of HDACi and enable them to be efficacious against solid tumors. We showed herein that morphing of folic and pteric acids into the surface recognition group of HDACi results in hydroxamate and benzamide HDACi which derived tumor homing by targeting folate receptor (FR), a receptor commonly overexpressed in solid tumors. We observed a correlation between the potency of HDAC1 inhibition and cytotoxicity as only the potent pterate hydroxamates, **11d** and **11e**, displayed antiproliferative activity against two representative FR-expression cancer cells. Our observation further supports the previous results which suggest that for a drug to be successfully targeted using the FR, it must be extremely potent against its primary target as the FR has a low delivery efficiency.

Published by Elsevier Masson SAS.

1. Introduction

Recent advances in cancer biology have led to the identification of novel targets for therapy [1,2]. Such targets include histone deacetylases (HDACs) which are components of the cellular epigenetic machinery [3–5]. There are 11 zinc dependent HDAC isoforms grouped into 3 classes (Classes I, II and IV) and 7 NAD⁺ dependent which form class III. Class I includes nuclear HDAC1, 2, 3 and 8. Isoforms 4, 5, 7 and 9 constitute the class IIa, which shuttle between the nucleus and the cytoplasm. The purely cytoplasmic

HDAC6 and 10 are members of class IIb, and HDAC11 represents the sole member of class IV. HDACs catalyze the removal of acetyl group from lysine residues of histone and non-histone proteins. Histone hypoacetylation causes chromatin condensation which concomitantly impedes the access of transcription factors to promoter segments within the condensed chromatin [3]. HDACs substrates are not limited to histone proteins. Other non-histone proteins whose activities are directly regulated by HDACs include HSP90, tubulin, androgen receptors, and p53 [6,7]. Moreover, the activity of the HDACs is opposed by histone acetyltransferases (HATs) which add acetyl group to lysine residues [3].

Due to their involvement in gene expression regulation, HDACs are recruited into various complexes by many cancers to purposely silence key pro-apoptotic genes. Consequently, specific HDAC isoforms are overexpressed in various cancer-types [8,9]. Inhibition of HDAC activity by broad spectrum inhibitors is now recognized as a novel treatment for certain cancers. Clinical trials have resulted in the FDA approvals of Vorinostat (SAHA) and Romidepsin (FK228) for the treatment of cutaneous T-cell lymphoma (CTCL) in 2006 and

Abbreviations: FR, Folate receptor; HDAC, Histone deacetylase; HDACi, Histone deacetylase inhibitor; ZBG, zinc binding group; SAR, structure activity relationship.

* Corresponding author. School of Chemistry and Biochemistry, Georgia Institute of Technology, Atlanta, GA 30332-0400, USA.

** Corresponding author. Department of Chemistry, Northwestern University, 2145 Sheridan Road, Evanston, IL 60208-3113, USA.

E-mail addresses: milan.mrksich@northwestern.edu (M. Mrksich), aoyelere@gatech.edu (A.K. Oyelere).

2009 respectively [10,11]. Like other anticancer drugs, HDACi have been associated with side effects including neutropenia, thrombocytopenia and potentially fatal cardiac arrhythmias [12]. In light of these shortcomings, HDACi therapy could benefit from a targeted therapeutic approach as it is the case for some currently available drugs [13]. Furthermore, this approach may address other deficiencies of HDACi, primarily their lack of efficacy towards solid tumors attributable to low therapeutic concentration within the malignant cells [14,15].

To meet their high metabolic demands, cancer cells overexpress various ligands receptors including those of vitamins [16,17]. Such receptors include the folate receptor (FR) whose expression is limited to certain epithelial cells including the choroid plexus, lung, thyroid, kidneys, and various malignancies [18–20]. This selective overexpression in cancer cells has made the FR an ideal candidate for targeted cancer therapy. FR mediated endocytic uptake of folate conjugates into malignant cells have been exploited for the delivery of diagnostic and therapeutic agents while minimizing delivery to

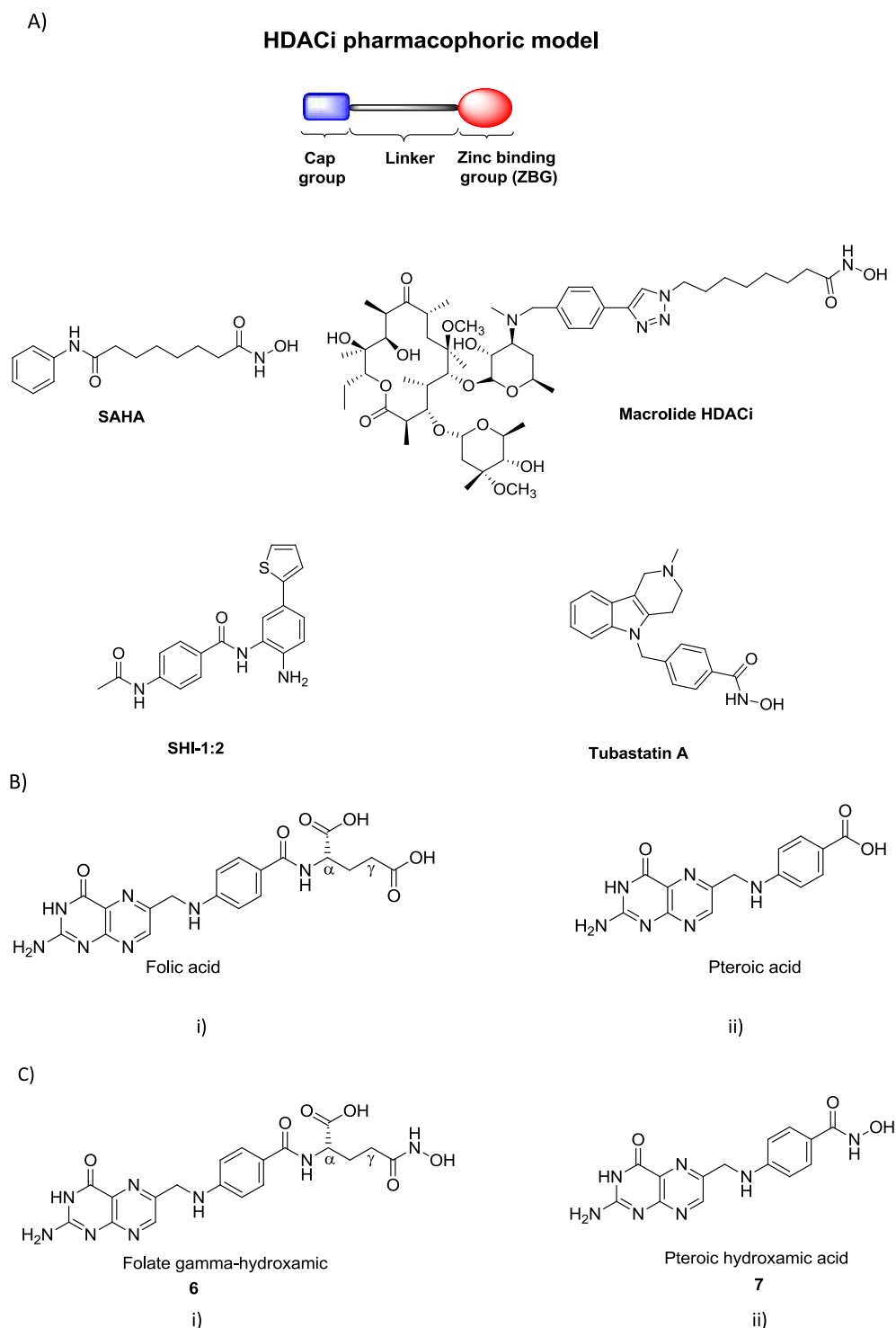


Fig. 1. HDACi pharmacophoric model and structures of selected HDACi A), folic acid (Bi), pteric acid (Bii), folate γ -hydroxamic acid (Ci) and pterate hydroxamic acid (Cii).

healthy cells [21–24]. Folate delivery to healthy cells is instead mediated by the ubiquitously expressed reduced folate carrier (RFC), which does not uptake folate conjugates [25,26]. Herein, we describe the design, synthesis and characterization of tumor-homing HDACi which derive their tumor selective accumulation from targeting the FR. We find that both folate and pterooate-based hydroxamates are potent inhibitors of HDAC1 and 6, but only the pterooic conjugated HDACi display anticancer activities against the folate receptor positive (FR+) tumors KB and HeLa. Moreover, HDAC1 inhibition is sufficient to induce apoptosis in KB cells whereas selective HDAC6 inhibition has no impact on KB cells survival.

2. Results and discussion

2.1. Design of folate receptor ligand-HDACi conjugates

Folic acid, which is comprised of pterooic acid and a glutamate residue (Fig. 1), has been commonly used to target the FR. Recent reports have however suggested that pterooic acid is also capable of mediating selective delivery of ligands to tumors overexpressing FR despite having minimal affinity for the FR [27–29]. Our main objective in this study is to investigate the prospect of folic and pterooic acids as mediators of selective delivery of HDACi to FR overexpressing cancer cells. To this end, we have designed a set of folate- and pterooate-HDACi conjugates in which the folate or pterooate moiety is integrated into the surface recognition group of a prototypical HDACi [3]. This design approach furnished minimally perturbed folate and pterooate analogs (Fig. 1C) and morphed folate-

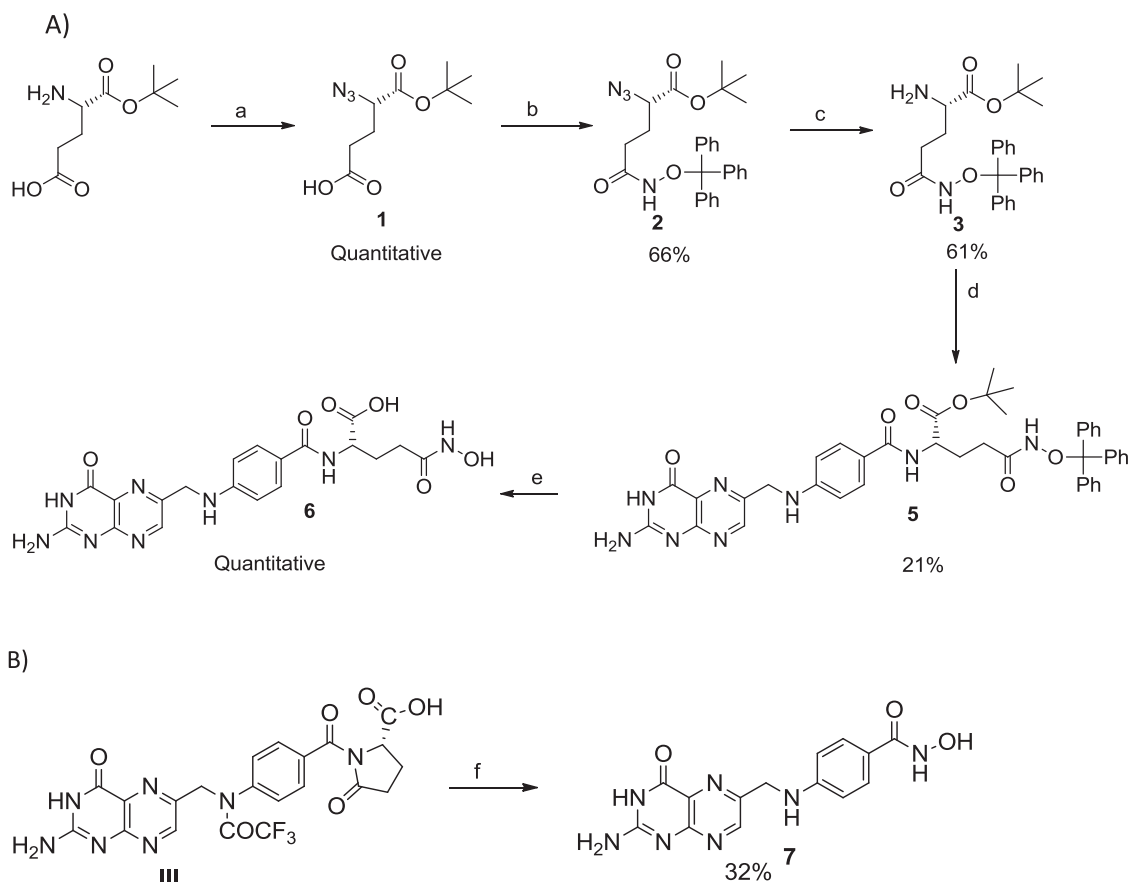
and pterooate-HDACi hybrids (Figs. 3, 5 and 7).

2.2. Synthesis and HDAC inhibition activity of folate γ -hydroxamic acid and pterooate hydroxamic acids

Due to the structural similarity of the pterooate group with typical HDACi surface recognition groups, we envisioned that the substitution of the carboxylic acid group of folic and pterooic acids with a zinc binding group (ZBG), essential for HDAC inhibition, would imbue tumor-homing functionality. Hence, the γ -carboxyl of folate and the carboxylate moiety of pterooic acid were converted to hydroxamic acid, the most commonly used ZBG for HDAC inhibition, to furnish compounds **6** and **7** respectively (Fig. 1C).

The reaction route for the synthesis of the folate γ -hydroxamate **6** and pterooate hydroxamate **7** is shown in Scheme 1. L-Glutamic acid α -tert-butyl ester was subjected to diazo-transfer resulting quantitatively in the α -azido L-glutamic acid α -tert-butyl ester **1** [30]. The α -azido glutamic acid **1** was coupled with O-tritylhydroxylamine in the presence of isobutylchloroformate (IBCF) and N-methyl-morpholine (NMM) resulting in compound **2** [31]. The azide moiety was then reduced to an amine with Zn and NH₄Cl yielding compound **3** [32]. The coupling of **3** with pteroyl azide **4** (see supporting info, Scheme S1 for the synthesis of **4**) in the presence of tetramethylguanidine (TMG) [33] resulted in the penultimate intermediate **5**. Exposure of this intermediate to trifluoroacetic acid (TFA) in the presence of trisopropylsilane (TIPS) yielded the desired folate γ -hydroxamate **6** (Scheme 1A) [34].

To obtain the pterooic hydroxamate **7**, N₁₀-(Trifluoroacetyl) pyrofollic acid (III, see Supporting info, Scheme S1), an intermediate



Scheme 1. Syntheses of folate γ -hydroxamate **6** (A) and pterooate hydroxamate **7** (B). a) TfN₃, K₂CO₃, CuSO₄·5H₂O, DCM, H₂O, MeOH, rt; b) IBCF, NMM, NH₂-O-trityl; c) NH₄Cl, Zn, EtOH/H₂O (3:1), reflux; d) Pteroyl azide (**4**), TMG, DMSO, rt; e) TFA, TIPS; f) 50% aqueous NH₂OH, DMSO, rt.

Table 1

Inhibition profile of folate γ -hydroxamic and pteroate hydroxamic acids (IC₅₀ in nM) against selected HDAC isoforms.

	HDAC1	HDAC6	HDAC8
Folate γ -hydroxamate (6)	^a NI	NI	NI
Pteroate hydroxamate (7)	2390 \pm 470	17.6 \pm 2.2	581 \pm 198

^a No significant inhibition (inhibition below 20% at 10 μ M).

in the synthesis of pteroyl azide **4** [33], was reacted with a 50% aqueous hydroxylamine in DMSO (Scheme 1B).

We then investigated the HDAC inhibition potential of the folate γ -hydroxamate **6** and pteroate hydroxamate **7** against HDAC1, 6, and 8 using the SAMDI mass spectrometry HDAC activity assay as previously described [35,36]. We observed that the folate γ -hydroxamate **6** was inactive against all three isoforms while the pteroate hydroxamate **7** inhibited these three HDACs. Compound **7** is particularly effective against HDAC6, with an IC₅₀ of 17.6 nM, and a selectivity enhancement of 130-fold relative to HDAC1 and 32-fold relative to HDAC8 (Table 1).

To obtain structural basis for the lack of HDAC inhibition by the folate γ -hydroxamate **6**, it was docked against homology models of HDAC1 and 6 built from human HDAC2 (PDB code: 3MAX) and HDAC8 (PDB code: 3FOR) respectively using Autodock 4.2 as previously described [35,36]. Against both isoforms, the folate γ -hydroxamate **6** adopts poses with the hydroxamate moiety pointing toward the active site Zn²⁺ ion, however it does so by positioning the α -carboxylate moiety in locations that are entropically unfavorable. With HDAC6, the α -carboxylate is inserted deep into the hydrophobic pocket where aromatic amino acids are located (Fig. 2i). The ensuing interactions may be unfavorable, potentially precluding the chelation of the hydroxamate moiety of **6** with the active site Zn²⁺ ion. Against HDAC1, compound **6** adopts different docked poses. Due to the narrowness of the channel leading to HDAC1 active site, the α -carboxylate is excluded from the channel and instead positioned in close proximity (<3 Å) to the carboxylate of ASP99 near the channel's entrance (Fig. 2ii). Electrostatic repulsion may then prevent the insertion of the ZBG into the active site.

2.3. SAR on pteroate-based hydroxamate HDACi

Unlike the folate γ -hydroxamate **6**, pteroate hydroxamate **7** was active against HDAC1, 6, and 8. To optimize its activity, we maintained the pteroate moiety as the surface recognition group but varied the length of the methylene linker separating it from

the ZBG (Fig. 3).

The synthesis of the pteroate hydroxamates **11a–g** is depicted in Scheme 2. Reduction of the previously described trityl azido hydroxamates **8a–g** with PPH₃ furnished the corresponding amines **9a–g** which were subsequently reacted with pteroyl azide **4** to yield the O-trityl protected hydroxamates **10a–g** [37,38]. The trityl protecting group was removed with TFA in presence of TIPS to give the requisite hydroxamates **11a–g** (Scheme 2) [34].

To evaluate the impact of the linker on their potency and isoform selectivity, we profiled the HDAC inhibition activity of hydroxamates **11a–g** against HDACs 1, 6 and 8 (Table 2). Relative to the “linker-less” compound **7**, the 3-methylene linker compound **11a** is a significantly weaker HDACi. Despite the loss of potency, however, **11a** is selective for HDAC6. Subsequent increases in the methylene linker length, up to 8-methylene groups largely resulted in improved HDAC1 and HDAC6 inhibition activities. We observed that a further increase in linker length is ultimately detrimental (Table 2, compare **11f** and **11g**). Among these pteroate hydroxamates, **11e** is the best HDAC1 inhibitor while **11f** is the best for HDAC6. Interestingly, we did not notice any glaring correlation between changes in the linker length and the HDAC8 inhibition activity of these pteroate hydroxamates.

To understand the basis of HDAC1 and HDAC6 inhibition by the pteroate-based hydroxamates, we docked **11a**, **11c** and **11e** against the homology model of HDAC1, whereas against the homology model of HDAC6, we docked **11a**, **11c** and **11f**. Zn²⁺ chelation seems to be the major determinant of HDAC inhibition against both isoforms. In HDAC1, the 3-carbon methylene linker of **11a** is not long enough to achieve optimal Zn²⁺ chelation (Fig. 4Ai). An increase to 5 carbon-methylene linker as in **11c** results in the close proximity of the ZBG to Zn²⁺ to achieve chelation. In addition to zinc chelation, **11e** is further stabilized by a T-shape interaction between its pterin ring and aromatic ring of TYR204 (Fig. 4Aii). Against HDAC6, all three compounds display optimal Zn²⁺ chelation (Fig. 4Bi), however, **11a** does not seem to be stabilized by any secondary interactions. On the other hand, the pterin moiety of **11c** and **11f** is involved in a π -stacking interaction with the aromatic ring of PHE680. The geometry of the π -stacking may explain the increased potency of **11f** compared to **11c** as the pterin ring in **11f** is ideally positioned for stacking with the phenyl ring of PHE680 (Fig. 4Bii).

2.4. Folate-based hydroxamate HDACi

Encouraged by the observed linker length dependence of the anti-HDAC activity of the pteroate hydroxamates, we revisited our

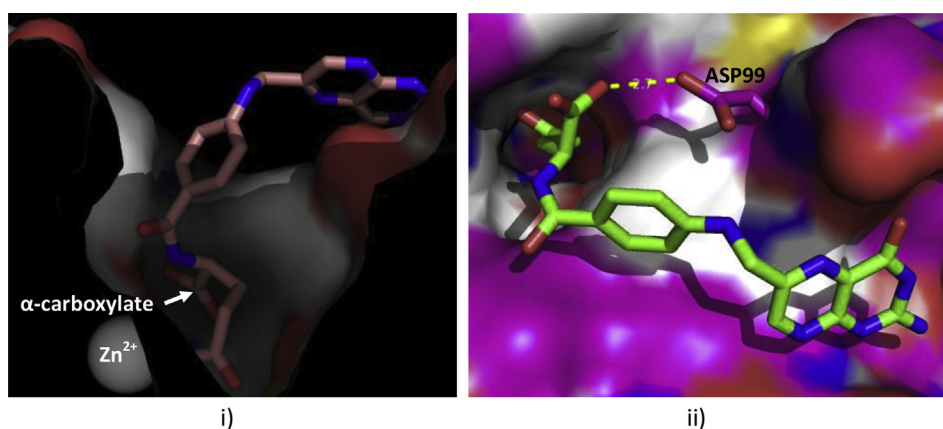


Fig. 2. Molecular docking studies explaining the lack HDAC inhibition by folate γ -hydroxamate **6**. The unfavorable interactions between the α -carboxylate of **6** and the enzymes active site residues preclude optimum chelation to the active site Zn²⁺ ion; i) In HDAC6: The α -carboxylate is inserted in the hydrophobic pocket; ii) HDAC1: The α -carboxylate of **6** is unable to enter the hydrophobic channel but is placed in close proximity to the carboxylate of ASP99.

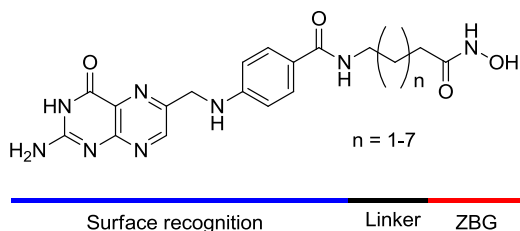


Fig. 3. Structure of Pteroate-based hydroxamates **11a–g**.

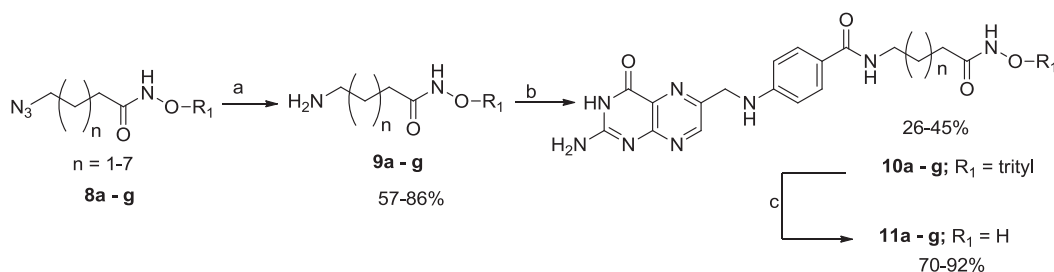
study on the folate series and performed similar structural alterations to the γ -carboxylate group of the folate template (Fig. 5). Additional impetus for studying folate-derived compounds may be the significantly enhanced affinity of folic acid, compared to their pteric acid congeners, for the FR. The synthesis of the folate-derived hydroxamates **15a–d** is depicted in Scheme 3. The α -azido L -glutamic acid α -tert-butyl ester **1** was coupled to the trityl amino hydroxamates **9a**, **9d**, **9e**, **9f** in the presence of IBCF and NMM to give the azido trityl protected hydroxamate compounds **12a–d** [31,39]. Subsequent azide reduction with NH_4Cl and Zn followed by coupling to the pteroyl azide **4** gave the protected folate based hydroxamate HDACi **14a–d** [32,33]. Removal of the trityl and t -Butyl protecting groups was accomplished in TFA with TIPS furnishing the desired folate based hydroxamate compounds **15a–d** [34].

Analogous to the pteroate series, compounds **15a–d** displayed linker length-dependent anti-HDAC activity with a clear preference for HDAC6 (Table 3). Against the three HDAC isoforms investigated, **15b** is the most potent among this series of HDACi. Relative to pteroate hydroxamates **11a–g**, compounds **15a–d** are generally less potent. However, selected members of this series – **15c** and **15d** – are more active against HDAC8 relative to their pteroate hydroxamate congeners **11e** and **11f**.

To understand the basis of the HDAC6 selectivity by the folate based hydroxamates, **15c** was docked against the homology models of HDAC1 and 6 built respectively from human HDAC2 (PDB code: 3MAX) and HDAC8 (PDB code: 3FOR) using Autodock 4.2 as previously described [35,36]. Against HDAC6, the hydroxamate ZBG of **15c** chelates to the zinc (Fig. 6Ai) and is stabilized by hydrogen bonds with the side chain of ASP567 and the C=O backbone of PHE566. Further stabilizing interactions may be attributed to the π -stacking interaction between the pterin ring and the phenyl ring of PHE680 (Fig. 6Aii). With HDAC1, zinc chelation is not optimal due to the following interactions obliging the hydroxamate ZBG to adopt the observed binding mode (Fig. 6Bi): hydrogen bonds with the side chains of GLU146, ASN95, ASP99, amide backbone of PHE205, as well as a T-shape interaction between the pterin ring and PHE205 (Fig. 6Bii).

2.5. Isoform selective folate based biaryl benzamide HDACi

Isoform selectivity of HDACi is believed to enhance the safety of



Scheme 2. Synthesis of Pteroate-based hydroxamates **11a–g**. a) PPh_3 , THF, rt; ii) H_2O ; b) Pteroyl azide **4**, TMG, DMSO, rt; c) TFA, TIPS.

Table 2

HDAC inhibition of Pteric based hydroxamates (IC_{50} in nM) against selected HDAC isoforms.

	n	HDAC1	HDAC6	HDAC8
11a	(1)	22.1 \pm 1.7%	1460 \pm 310	25 \pm 18%
11b	(2)	6150 \pm 1320	212 \pm 15	39 \pm 6%
11c	(3)	79.6 \pm 12.6	43.6 \pm 8.4	41 \pm 17%
11d	(4)	23.4 \pm 4.2	12.2 \pm 0.2	1060 \pm 320
11e	(5)	16.1 \pm 2.8	55.4 \pm 2.2	9380 \pm 1720
11f	(6)	524 \pm 36	10.2 \pm 1.0	7590 \pm 2120
11g	(7)	53 \pm 7%	476 \pm 48	40 \pm 10%
SAHA	–	38 \pm 2	144 \pm 23	232 \pm 19

% inhibition at 10 μM are given if the IC_{50} was above 10 μM .

HDACi therapy based in part on the observation that the class I selective inhibitor MS275 and the HDAC6 selective inhibitor ACY-1215 are well tolerated in clinical trials [3,40]. We incorporated benzamide, which is a known HDAC1-selective ZBG, into the design of the folate based compounds (Fig. 7).

Precursor of the biaryl benzamide ZBG **16** was synthesized as previously reported [41]. The biaryl benzamide ZBG **17** was obtained following the reduction of the nitro group in presence of Zn in dioxane/ H_2O (4:1) (Scheme 4) [42]. In presence of EDCI and HOBT, the ZBG **17** was coupled to various azido carboxylic acids (**18a–d**) to give compounds **19a–d** [31,37]. Following the reduction of the azide **19a–d** with zinc and NH_4Cl , the resulting compounds **20a–d** were coupled to α -azido glutamic acid **1** to give intermediates **21a–d**. Zinc-mediated reduction of **21a–d** gave **22a–d** which were coupled with pteroyl azide **4** to give the penultimate intermediates **23a–d**. Final removal of protecting groups with TFA containing TIPS affords the desired folate based biaryl benzamide HDACi **24a–d** (Scheme 4) [34].

In contrast to their hydroxamate congeners, the biaryl benzamides **24a–d** are devoid of HDAC6 and 8 inhibition. However, they show chain length-dependent HDAC1 inhibition from the minimally potent 3-methylene linker **24a** to the highly potent 7-methylene spacer **24c** (Table 4). This HDAC1 selectivity is expected as the biaryl benzamide ZBG is selective for HDAC1 [41].

2.6. Anticancer activity of pteroate and folate-derived HDACi

Most HDACi are inherently incapable of targeting tumor cells, and they therefore have off-target toxic effects [3]. Tumor cell-selective uptake of HDACi could potentially ameliorate many of their shortcomings. To evaluate the influence of the FR on the cytotoxic activity of the folate- and pteroate-derived HDACi

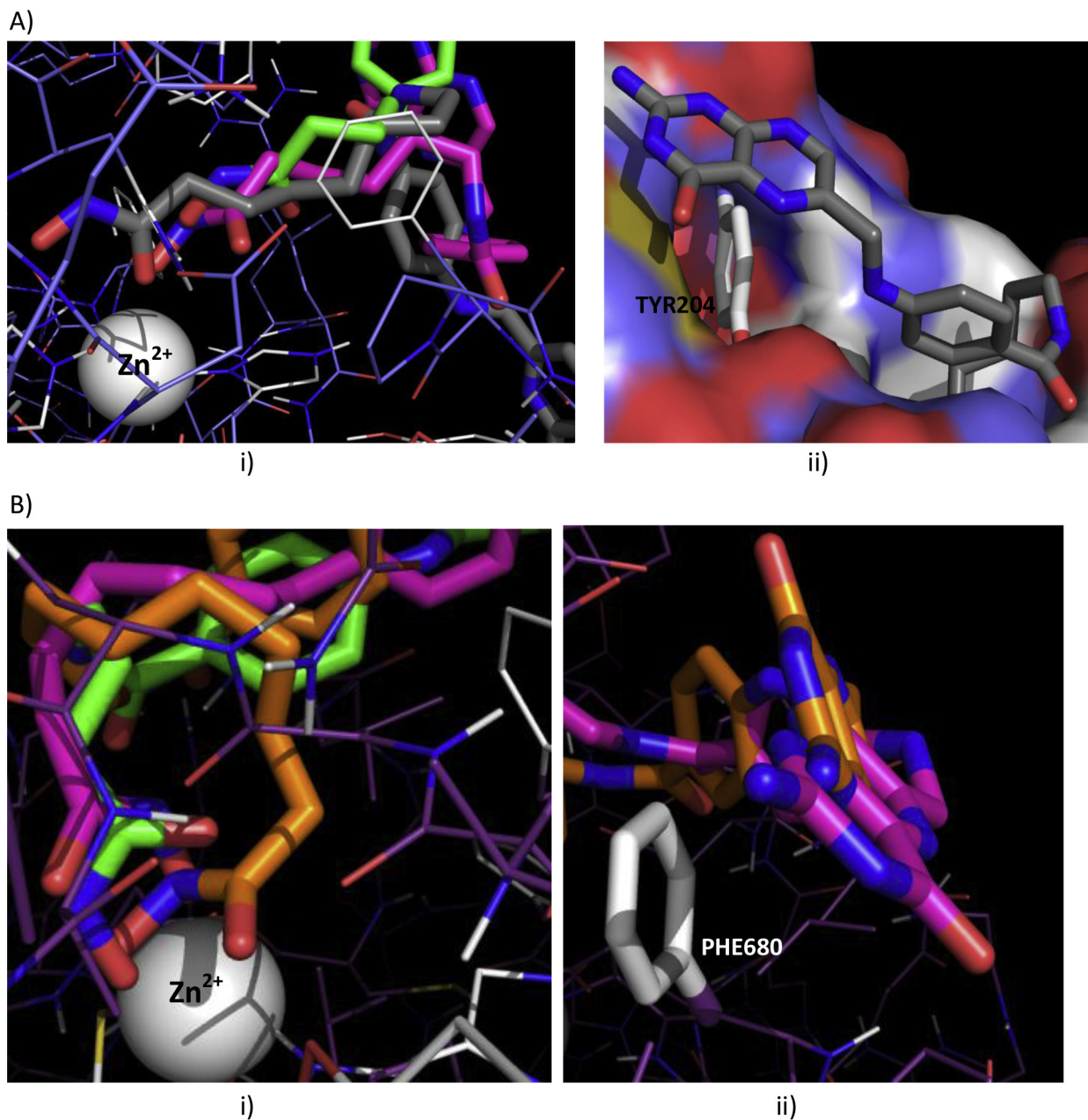


Fig. 4. Molecular docking poses explaining the inhibitory profile of selected pteroate-based hydroxamates against HDAC1 and HDAC6; A) **HDAC1**: i) Both **11c** (purple) and **11e** (gray) chelate the active site Zn^{2+} but **11a** (green) does not due to a short linker; ii) In addition to Zn^{2+} chelation, **11e** (gray) is further stabilized by a T-shape interaction between its pterin and the aromatic ring of TYR204. B) **HDAC6**: i) All three inhibitors, **11a** (green), **11c** (purple) and **11f** (orange) chelate the Zn^{2+} ; ii) Both **11c** and **11f** are further stabilized by a π -stacking between their respective pterin ring and PHE680, furthermore the pterin ring of **11f** is ideally positioned for stacking with the aromatic ring of PHE680 unlike in **11c**. (For interpretation of the references to color in this figure legend, the reader is referred to the web version of this article.)

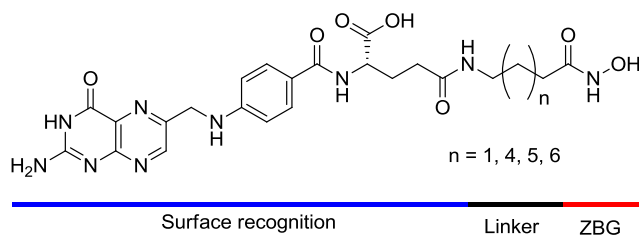
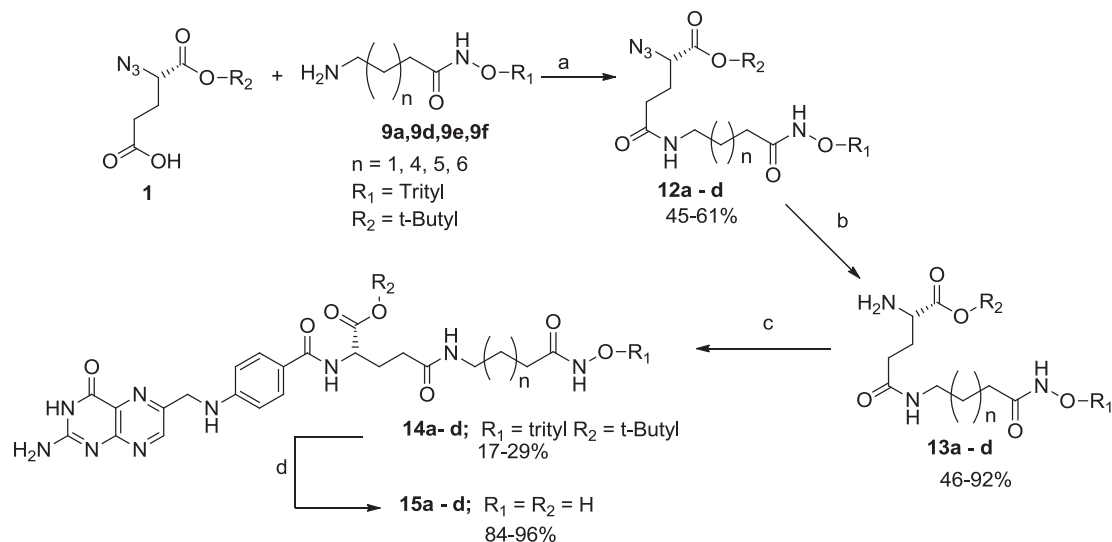


Fig. 5. Structure of folate based hydroxamates **15a–g**.

identified above, we investigated the effects of their exposure on the viability of two FR (+) transformed cell lines, KB (oral carcinoma) and HeLa (cervical carcinoma) cells [43]. We observed that none of the folate-based hydroxamates and biaryl benzamides were active against either cell lines. Among the pteroate hydroxamates, only the 6- and 7-methylene linker **11d** and **11e**, respectively, were active with micromolar IC_{50} s (Table 5). KB cells were more responsive to these compounds as reflected by the lower IC_{50} compared to those in HeLa cells. This observed difference in sensitivity is in agreement with previous observations since HeLa cells have a lower FR density than the KB cells [44].

To confirm the FR as the route of entry of the pteroate-based hydroxamates into the KB cells, we measured the cell viability in



Scheme 3. Synthesis of folate based hydroxamates. a) IBCF, NMM; b) Zn, NH_4Cl , $\text{EtOH}/\text{H}_2\text{O}$ (3:1), reflux; c) Pteroyl azide **4**, TMG, DMSO, rt; d) TFA, TIPS.

the presence and absence of folic acid as previously described [45]. The addition of folic acid (250 μM) reduced the cytotoxicity of **11e** (Fig. 8). Furthermore, we observed that both **11d** and **11e** are inactive against the FR (–) lung cancer cell line A549. These results suggest a reliance on the FR for the cellular uptake of the pteroate hydroxamate compounds [46].

2.7. Validation of intracellular targets

Inhibition of HDAC1 or 6 have been associated with the anti-proliferative activities of HDACi [41,47,48]. The most potent HDAC6 selective inhibitor in the series disclosed herein is the pteroate hydroxamate **7** (Table 1). However, compound **7** is not cytotoxic to the KB and HeLa cells up to 100 μM . The lack of cytotoxic activity of **7** may suggest that HDAC6 inhibition does not lead to KB cell death. Alternatively, it may be that **7** is unable to penetrate KB cell. However, when docked against the FR crystal structure (PDB code: 4LRH), **7** binds to the FR, and its pterin moiety is involved in stabilizing interactions similar to the interactions between the active lead-compounds **11d** and **11e** and the FR. Furthermore, the interactions between the pterin ring of compounds **7**, **11d**, **11e** and the FR are analogous to those previously reported between folic acid and FR (Fig. 9). This structural information suggests that the

pteroate hydroxamate **7** and active lead-compounds **11d** and **11e** are capable of productive interaction with FR and this may lead to their FR-dependent cell uptake [49].

We used immunoblotting to investigate the cell response to compounds **7**, **11d**, and **11e**. First, we monitored tubulin acetylation as a marker of HDAC6 activity in KB cells and included the pan-inhibitor SAHA as a control [50]. As expected, SAHA and the lead-compounds **11d** and **11e** induced an increase in acetylated tubulin levels at IC_{50} doses and above, thereby confirming HDAC6 as a target (Fig. 10). Interestingly, a similar increase in tubulin acetylation was observed upon cell exposure to pteroate hydroxamate **7** (100 μM) (Fig. 10). This finding suggests that the selective HDAC6 inhibitor **7** is indeed targeting intracellular HDAC6. Because compound **7** is non-cytotoxic, it appears that HDAC6 inhibition is not entirely detrimental to the viability of KB cells.

To further exclude the contribution of HDAC6 inhibition to the mechanism of cytotoxicity, we investigated the effects of the HDAC6-selective inhibitor Tubastatin A [51] and HDAC1-selective inhibitor biaryl benzamide SHI-1:2 [41] on KB cell survival. We observed that the HDAC1 selective SHI-1:2 potently inhibits cell proliferation with an IC_{50} of $5.27 \pm 0.84 \mu\text{M}$. Tubastatin A was also cytotoxic but less potent with an IC_{50} of $14.81 \pm 2.74 \mu\text{M}$. Thus, it would be easy to conclude that HDAC6 activity is essential to viability. However, the high concentration of Tubastatin A required for cell death approximate its *in vitro* IC_{50} for HDAC1 ($16.4 \pm 2.6 \mu\text{M}$) [51]. Therefore, the observed cytotoxicity of Tubastatin A to the KB cells may largely be derived from HDAC1 inhibition. To verify the plausibility of this scenario, we used KB cells to determine the effect of Tubastatin A, together with pteroate hydroxamates **7**, **11d**, **11e**, and SAHA, on the acetylation status histone H4, an intracellular marker of HDAC1 inhibition [50]. As expected, SAHA, **11d**, and **11e** displayed dose dependent increases in histone H4 acetylation (Fig. 11). At 14 μM , Tubastatin A also showed a significant increase in H4 acetylation. This observation further supports the involvement of intracellular HDAC1 inhibition as the major contributor to the cytotoxic activity of Tubastatin A against KB cells. Interestingly, pteroate hydroxamate **7** at 100 μM has little effect on H4 acetylation relative to the control (Fig. 11, compare lanes 1 and 8), supporting its selectivity for HDAC6 and further explaining why it is non-cytotoxic at this concentration.

Finally, the correlation between HDAC1 inhibition and KB cell viability may explain the lack of anticancer activity of the folate

Table 3
 HDAC inhibition of folate based hydroxamates (IC_{50} in nM) against selected HDAC isoforms.

	n	HDAC1	HDAC6	HDAC8
15a	(1)	NI	8050 \pm 330	40 \pm 5%
15b	(4)	1770 \pm 100	132 \pm 23	2390 \pm 640
15c	(5)	1800 \pm 180	193 \pm 41	2370 \pm 430
15d	(6)	2760 \pm 550	179 \pm 19	1560 \pm 340
SAHA	–	38 \pm 2	144 \pm 23	232 \pm 19

% inhibition at 10 μM are given if the IC_{50} was above 10 μM .

NI: No significant inhibition (below 20% Inhibition at 10 μM concentration).

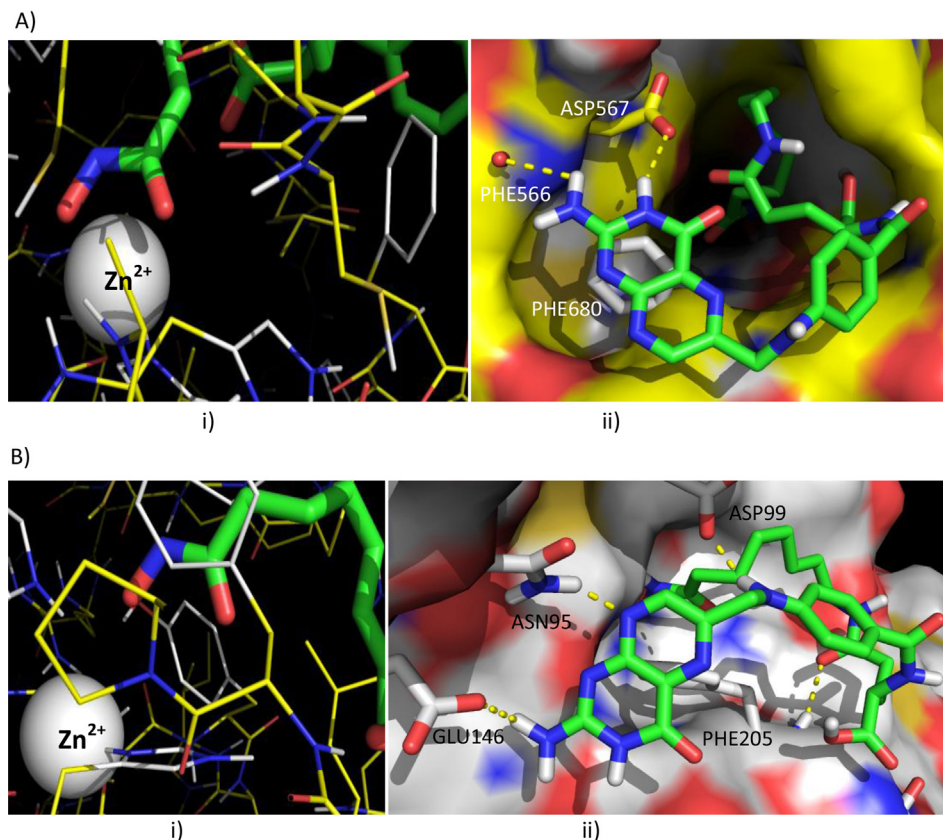


Fig. 6. Molecular basis for isoform selectivity of **15c**. A) Molecular docking of **15c** with HDAC6 homology model built from HDAC8 (PDB code: 3FOR); i) Zinc chelation by **15c**; ii) Polar interactions between **15c** and HDAC6 homology model and π -stacking of phenyl of PHE680 with **15c**; B) Molecular docking of **15c** with HDAC1 homology model built from HDAC2 (PDB code: 3MAX); i) Orientation of the hydroxamate ZBG at the active site; ii) Stabilizing interactions between **15c** and HDAC1 homology model include H-bonds and T-shape interaction of PHE205 with pterin ring of **15c**.

based hydroxamate compounds, since they are poor HDAC1 inhibitors (Table 3). However, the inactivity of the HDAC1-inhibitors folate-based biaryl benzamides **24a–d** (Table 4) against KB cells may be contrary to this correlation. In an attempt to resolve this apparent contradiction, we speculated that the biaryl benzamide ZBG may be perturbing FR binding. However, molecular docking studies of **24b** and **24c** revealed that the binding interactions with the FR were similar to folic acid (Fig. 12), suggesting that the ZBG may not be perturbing the stabilizing interactions between these compounds and the FR. Recent studies have shown that a proton-coupled folate transporter (PCFT) is responsible for the export of folates from endosomes following endocytosis [52]. The folate-based biaryl benzamides may not be efficiently transported by the PCFT leading to their retention in the endosomes upon endocytosis. Although the folate receptor has been successfully targeted for the delivery of therapeutic agents, observations made by Philip Low's group revealed that only 15–25% of the bound FR release

their substrates following endocytosis, the rest of the bound receptors are returned to the cell surface [22]. Thus, targeting by FR binding may require relatively potent leads to compensate for the fractions that remain bound [21]. This may explain why the relatively more potent compounds **11d** and **11e** (Table 2) are cytotoxic, while the less potent **24a–d** are not.

3. Conclusion

Despite success against hematological malignancies, HDACi have not been effective against solid tumors. Targeting HDACi directly to tumors, however, may enhance their therapeutic utility. Prior attempts have exploited the folate receptor, which is over-expressed in some tumors, as a Trojan horse for delivery by conjugating HDACi to folate [45,53]. While these compounds indicate HDACi inhibition, there is little indication of FR involvement for cellular uptake [53]. A direct conjugate of folic acid to common thiolate HDACi unfortunately abolishes HDAC inhibition activity [45]. We show that morphing of folic and pteric acids into the surface recognition group of certain hydroxamate and benzamide HDACi yields isoform selective HDACi that target the FR. We observed that the benzamide HDACi are HDAC1 selective while the pterate-based hydroxamates are potent inhibitors of HDAC1 and 6. Furthermore, we established a correlation between the potency of HDAC1 inhibition and cytotoxicity, as only the pterate hydroxamates **11d** and **11e** harboring low nanomolar HDAC1 inhibition activity displayed antiproliferative activity against KB and HeLa cells. While the folate receptor is a promising conduit for targeted therapy, its low delivery efficiency may constitute an

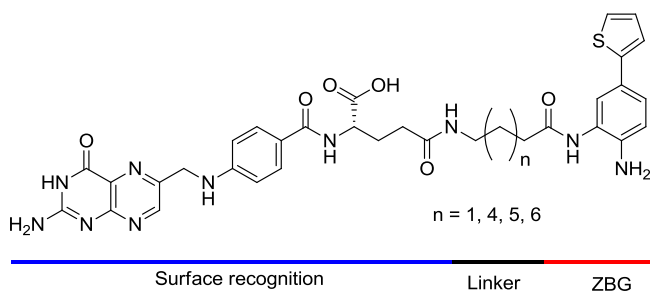
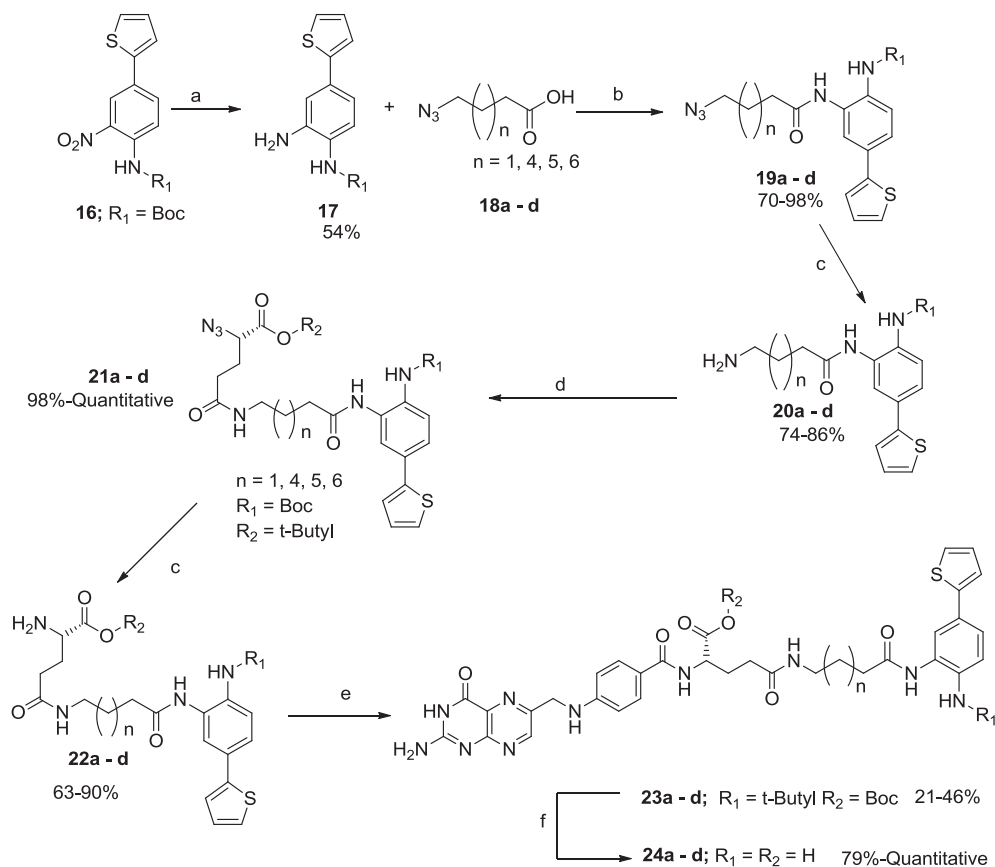


Fig. 7. Structure of folate based biaryl benzamide HDACi.



Scheme 4. Synthesis of folate based biaryl benzamide HDACi. a) Zn, Dioxane/H₂O (4:1), 70 °C; b) EDCI, HOBT, DMF, 70 °C; c) Zn, NH₄Cl, EtOH/H₂O (3:1), reflux; d) **1**, EDCI, HOBT, DMF, rt; e) Pteroyl azide **4**, TMG, DMSO; f) TFA, TIPS.

obstacle. Our observations support the notion that targeting by way of the folate receptor requires that drugs are very potent against their primary targets.

4. Experimental section

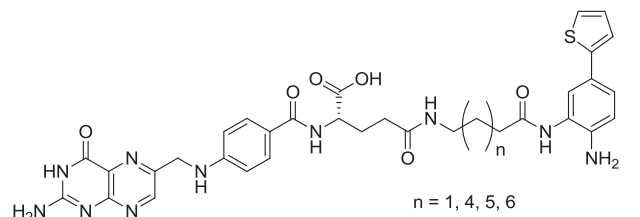
4.1. Materials and methods

Folic acid and other reagents used were purchased from Sigma–Aldrich (St. Louis, MO, USA) and Alfa Aesar (WardHill, MA, USA). Analtech silica gel plates (60 F₂₅₄) were used for analytical TLC, and Analtech preparative TLC plates (UV 254, 2000 μm) were used for purification. UV light was used to examine the spots. Silica gel (200–400 Mesh) was used in column chromatography. NMR spectra were recorded on a Varian–Gemini 400 magnetic resonance spectrometer. ¹H NMR spectra were recorded in parts per million (ppm) relative to the peak of CDCl₃, (7.24 ppm), CD₃OD (3.31 ppm), or DMSO-*d*₆ (2.49 ppm). ¹³C spectra were recorded relative to the central peak of the CDCl₃ triplet (77.0 ppm), CD₃OD (49.0 ppm), or the DMSO-*d*₆ septet (39.7 ppm), and were recorded with complete heterodecoupling. Multiplicities are described using the abbreviation s, singlet; d, doublet; t, triplet; q, quartet; m, multiplet; and app, apparent. High-resolution mass spectra were recorded at the Georgia Institute of Technology mass spectrometry facility in Atlanta. KB and A549 cells were obtained from ATCC (Manassas, VA, USA), HeLa cell line was kindly donated by Dr. Christoph Farhni and grown on folate free RPMI medium supplemented with 10% fetal bovine serum (Global Cell Solutions, Charlottesville, VA, USA) and 1% pen/Strep (Cellgro, Manassas, VA) at 37 °C in an incubator with 5% CO₂. Mouse anti-acetylated α-Tubulin antibody was obtained

from Invitrogen (Life Technologies, Grand Island, NY, USA), rabbit anti-actin, rabbit anti-tubulin α, rabbit anti-histone H4 antibodies and Tubastatin A were purchased from Sigma–Aldrich (St. Louis, MO, USA). Secondary antibodies, goat anti-rabbit conjugated to IRDye680 and goat anti-mouse conjugated to IRDye800 were purchased from LI-COR Biosciences (Lincoln, NE, USA). The CellTiter 96 Aqueous One Solution Cell Proliferation assay (MTS) kit was purchased from Promega (Madison, WI, USA).

Table 4

HDAC inhibition of folate based biaryl benzamides (IC₅₀ in nM) against selected HDAC isoforms.

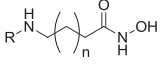


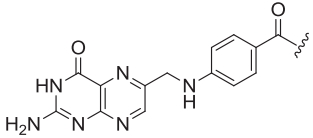
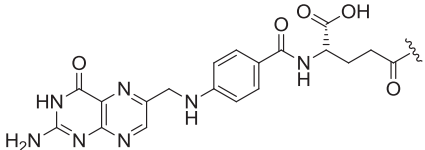
	n	HDAC1	HDAC6	HDAC8
24a (C4)	(1)	2940 ± 330	22.8 ± 0.3%	23 ± 6%
24b (C7)	(4)	435 ± 35	NI	NI
24c (C8)	(5)	287 ± 53	NI	≈ 10,000
24d (C9)	(6)	309 ± 74	NI	NI
SAHA	–	38 ± 2	144 ± 23	232 ± 19

% inhibition at 10 μM are given if the IC₅₀ was above 10 μM.

NI: No significant Inhibition (below 20% Inhibition at 10 μM concentration).

Table 5
Folate receptor-dependent anti-proliferative activity of folate- and pterate-derived hydroxamates (IC₅₀ in μM).



R	n	KB	HeLa	A549	
	11a	1	NI	NI	NT
	11b	2	NI	NI	NT
	11c	3	25 ± 2%†	NI	NT
	11d	4	53.7 ± 2.4	34 ± 3%†	NI
	11e	5	30.3 ± 2.1	56.6 ± 1.1	NI
	11f	6	33 ± 3%†	35 ± 3%†	NT
	11g	7	47 ± 3%†	36 ± 8%†	NT
	15a	1	NT	NT	NT
	15b	4	NI	NI	NT
	15c	5	NI	NI	NT
	15d	6	NT	NT	NT
SAHA	—	1.8 ± 0.3	3.7 ± 0.2	NT	

NI: No inhibition (below 20% inhibition at 100 μM); †: % inhibition at 100 μM ; NT: Not tested.

4.2. Histone deacetylase inhibition assay

The HDAC activity in presence of various compounds was assessed by SAMDI mass spectrometry as described [54]. To obtain IC₅₀ values, we incubated isoform-optimized substrates (50 μM , detailed below) with enzyme (250 nM, detailed below) and inhibitor (at concentrations ranging from 10 nM to 1.0 mM), in HDAC buffer (25.0 mM Tris–HCl pH 8.0, 140 mM NaCl, 3.0 mM KCl, 1.0 mM MgCl₂, 0.1 mg/mL BSA) in 96-well microtiter plates (60 min, 37 °C). Solution-phase deacetylation reactions were quenched with trichostatin A (TSA) and transferred to SAMDI plates to immobilize the substrate components. SAMDI plates were composed of an array of self-assembled monolayers (SAMs) presenting maleimide in standard 384-well format for high-throughput handling capability. Following immobilization, plates were washed to remove buffer constituents, enzyme, inhibitor, and any unbound substrate and analyzed by MALDI mass spectrometry using automated protocols [55]. Deacetylation yields in each triplicate sample were determined from the integrated peak intensities of the molecular ions for the substrate and the deacetylated product ion by taking

the ratio of the former over the sum of both. Yields were plotted with respect to inhibitor concentration and fitted to obtain IC₅₀ values for each isoform–inhibitor pair.

Isoform-optimized substrates were prepared by traditional Fmoc solid phase peptide synthesis (reagents supplied by Anaspec) and purified by semi preparative HPLC on a reverse phase C18 column (Waters). The peptide of sequence GRK^{ac}FGC was prepared for HDAC1 and HDAC8 experiments, while the peptide of sequence GRK^{ac}YGC was prepared for HDAC6 experiments. Isoform preference for the indicated substrates was determined by earlier studies on peptide arrays [54].

HDAC1 and HDAC6 were purchased from BPS Biosciences. The catalytic domain of HDAC8 was expressed as previously reported [54]. Briefly, an amplicon was prepared by PCR with the following primers: forward 5'-3' TATTCTCGAGGACCACATGCTTCA and reverse 5'-3' ATAAGCTAGCATGGAGGAGCCGGA. A pET21a construct bearing the genetic insert between NheI and XhoI restriction sites was transformed into *Escherichia coli* BL21(DE3) (Lucigen) and expressed by standard protocols. Following purification by affinity chromatography, the His-tagged enzyme-containing fractions were purified by FPLC (AKTA) on a superdex size exclusion column (GE), spin concentrated, and stored at –80 °C in HDAC buffer with 10% glycerol.

4.3. Molecular docking analysis

The docking studies were performed as previously reported with Autodock Vina through PyRx [56,57]. Following the 3D energy minimization of the ligand by ChemBioDraw 3D, the docking was run in a 25 Å cubic space surrounding the active site, the binding pocket.

4.4. Cell viability assay

KB and HeLa cells were maintained in folate free-RPMI supplemented with 10% FBS and 1% pen/strep while A549 cells were maintained in DMEM supplemented with 10% FBS and 1% pen/strep. All cells were incubated on a 96-wells plate in folate free-RPMI for 24 h prior to a 72 h drug treatment. Cell viability was measured using the MTS assay according to manufacturer protocol. The DMSO concentration in the cell media during the cell viability experiment was maintained at 0.1%.

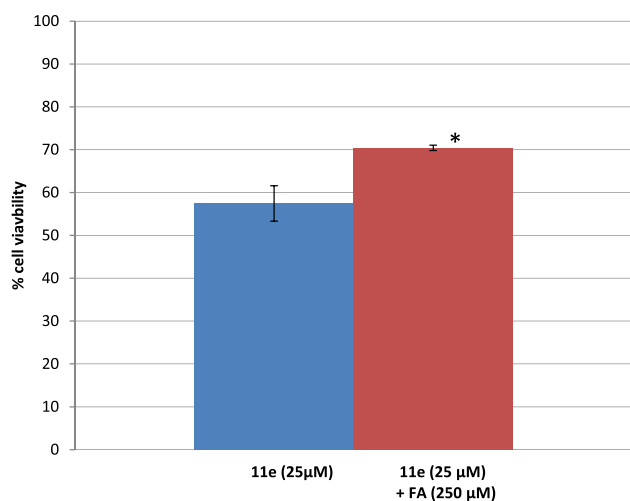


Fig. 8. Folic acid (FA) competition assay. Viability of KB cells treated with 25 μM of **11e** in the absence and presence of FA. * $p < 0.01$ (Student's *t*-test).

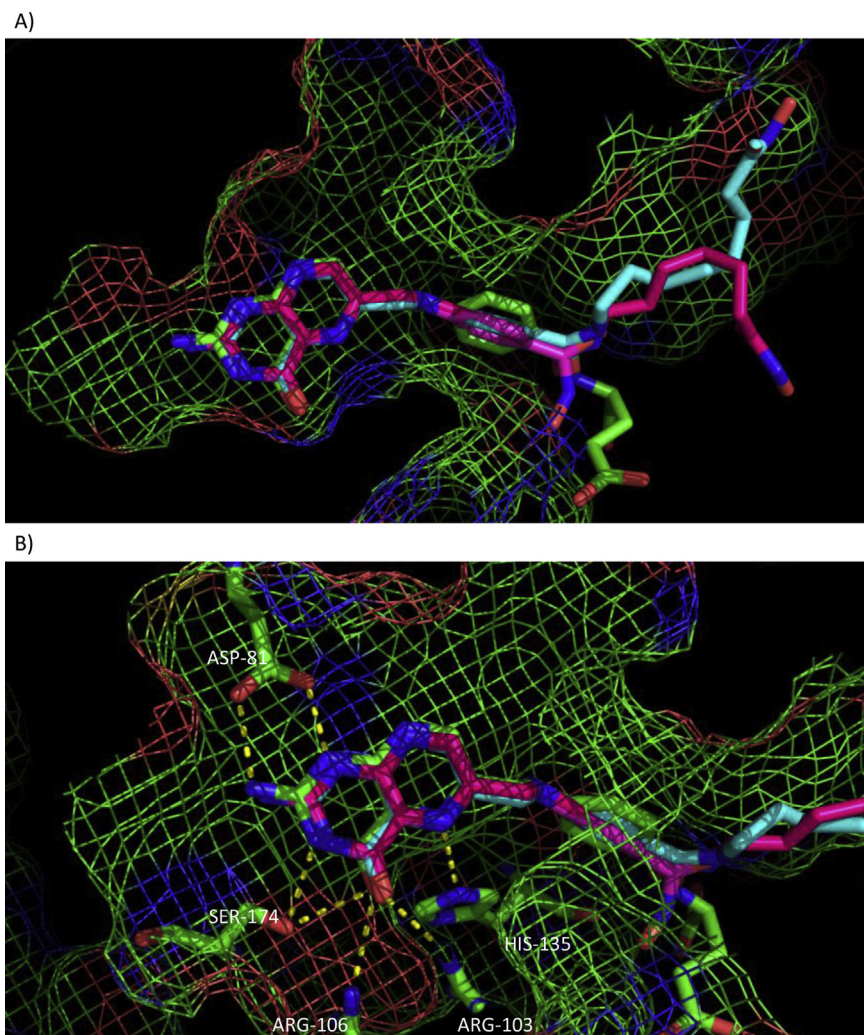


Fig. 9. Molecular docking of the FR (PDB code: 4LRH) against folic acid (green), Pteroate hydroxamate **7** (purple), **11d** (pink) and **11e** (blue). A) The pterin ring of pteroate hydroxamate **7**, **11d** and **11e** have a similar binding mode to the ligand binding pocket as folic acid. B) Stabilizing interactions between the FR and the pterin ring of Pteroate hydroxamate **7**, **11d** and **11e** are analogous to those reported for the interaction between the FR and folic acid [49]. (For interpretation of the references to color in this figure legend, the reader is referred to the web version of this article.)

4.5. Western blot analysis for tubulin and histone H4 acetylation

KB cells were plated for 24 h and treated with various concentrations of compounds for 4 h (tubulin acetylation) or 24 h (histone H4 acetylation). Cells were washed with PBS buffer and resuspended in CellLyctic™ buffer containing a cocktail of protease inhibitor (Sigma–Aldrich, St. Louis, MO, USA). Following the protein quantification using a Bradford protein assay, equal amount of protein was loaded onto an SDS-page gel (Bio-Rad, Hercules, CA, USA) and resolved by electrophoresis at a constant voltage of 100 V

for 2 h. The gel was transfer onto a nitrocellulose membrane and probed for acetylated tubulin, tubulin, acetylated histone H4, histone H4 and actin.

4.6. Statistical analysis

The values reported as mean \pm standard deviation from at least 2 independent triplicate experiments. A student's t-test was performed in Excel, and results with p value less than 5% were considered statistically different.

4.7. Synthesis of compounds

4.7.1. Trifluoromethanesulfonyl azide (TfN₃)

The title compound was synthesized according to previous protocol [58]. Briefly, NaN₃ (1.36 g, 20.86 mmol) was dissolved in DCM (7.5 mL) and H₂O (4.5 mL) and cooled in an ice bath. Upon addition of triflyl anhydride (0.71 mL, 4.17 mmol) dropwise, the reaction was stirred at room temperature for 2 h. The DCM layer was removed using a separatory funnel and the aqueous layer was extracted with DCM (2 \times 4 mL). The organic layers were combined and washed with Na₂CO₃ and dried with Na₂SO₄. The crude product

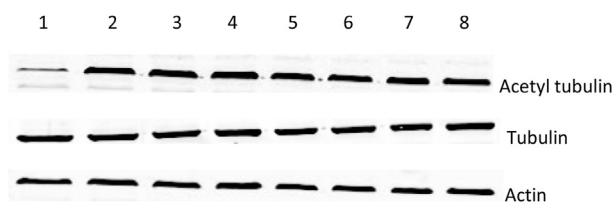


Fig. 10. Western blot analysis of tubulin acetylation in KB cells. 1) Control; 2) SAHA (2 μ M); 3) SAHA (20 μ M); 4) **11d** (50 μ M); 5) **11d** (100 μ M); 6) **11e** (30 μ M); 7) **11e** (100 μ M); 8) **7** (100 μ M).

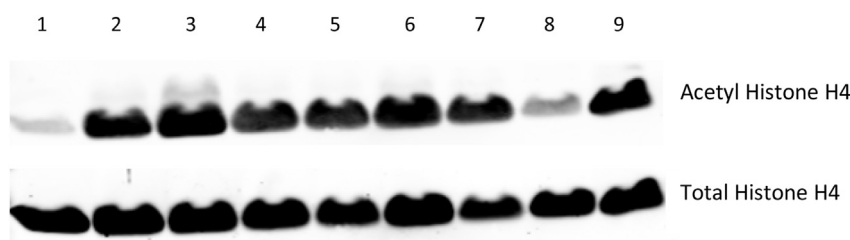


Fig. 11. Western blot analysis of Histone H4 acetylation in KB cell. 1) Control; 2) SAHA (2 μ M); 3) SAHA (20 μ M); 4) **11d** (50 μ M); 5) **11d** (100 μ M); 6) **11e** (30 μ M); 7) **11e** (100 μ M); 8) **7** (100 μ M); 9) Tubastatin A (14 μ M).

was used without further purification.

4.7.2. (*S*)-4-Azido-5-(*tert*-butoxy)-5-oxopentanoic acid (**1**)

L-Glutamic acid α -*tert*-butyl ester (0.5 g, 2.09 mmol), K_2CO_3 (0.43 g, 3.13 mmol), and $CuSO_4 \cdot 5H_2O$ (0.0050 g, 0.021 mmol) were dissolved in MeOH (18 mL) and H_2O (9 mL). The previously synthesized TfN_3 in DCM was added and the mixture was stirred overnight at room temperature. The organic solvents were evaporated off and the aqueous layer was acidified to pH 2 with a 2 M HCl solution and extracted with DCM (4×20 mL). The DCM extracts were combined, washed with brine and dried with Na_2SO_4 . Evaporation of the DCM resulted in **1** (0.52 g, quantitative yield). 1H NMR (400 MHz, $CDCl_3$) δ 3.85 (dd, $J = 8.7, 5.2$ Hz, 1H), 2.47 (t, $J = 6.8$ Hz, 2H), 2.17–2.04 (m, 1H), 2.01–1.88 (m, 1H), 1.47 (d, $J = 1.5$ Hz, 9H). ^{13}C NMR (101 MHz, $CDCl_3$) δ 178.6, 169.0, 83.4, 61.4, 29.9, 27.9, 26.1.

4.7.3. (*S*)-*Tert*-butyl 2-azido-5-oxo-5-((trityloxy)amino)pentanoate (**2**): representative procedure for amide bond formation through a mixed anhydride intermediate

A THF solution of **1** (0.49 g, 2.15 mmol) and *N*-methylmorpholine (0.22 g, 2.15 mmol) was cooled to $-15^\circ C$ and stirred for 5 min. Isobutylchloroformate (0.29 g, 2.15 mmol) was added and the mixture stirred at $-15^\circ C$ for 10 min. *O*-Tritylhydroxylamine (1.19 g, 4.30 mmol) and *N*-methylmorpholine (0.44 g, 4.30 mmol) were added and the reaction was stirred at $-15^\circ C$ for 15 min and at room temperature for 2 h. Upon reaction completion, DCM (100 mL) was added and the mixture was washed with approx. 50 mL of H_2O , 50 mL of $NaHCO_3$ (1 \times), 50 mL of 1 M HCl (1 \times), 50 mL of brine (1 \times)

and dried with Na_2SO_4 . Following the evaporation of the organic layer, the crude product was dissolved in EtOAc and addition of Hexanes resulted in the precipitation of the product **2** as a white solid (0.69 g, 66% yield). 1H NMR (400 MHz, $CDCl_3$) δ 7.61–7.28 (m, 15H), 3.66–3.49 (m, 1H), 2.06–1.91 (m, 1H), 1.80–1.66 (m, 2H), 1.62–1.55 (m, 1H), 1.46 (s, 9H). ^{13}C NMR (101 MHz, $cdcl_3$) δ 175.8, 169.2, 141.8, 141.0, 129.1, 128.2, 93.6, 82.8, 61.6, 28.0, 27.4, 25.3.

4.7.4. (*S*)-*Tert*-butyl 2-amino-5-oxo-5-((trityloxy)amino)pentanoate (**3**): representative procedure for azide reduction to amine using Zn and NH_4Cl

To a solution of **2** (0.25 g, 0.51 mmol) in EtOH (3 mL) and H_2O (1 mL), NH_4Cl (0.066 g, 1.23 mmol) and zinc powder (0.047 g) were added and the resulting mixture was stirred under reflux for 2 h. After completion of the reaction, the mixture was filtered through a celite pad. Following the removal of the solvent, the crude product was purified by preparative TLC with DCM:MeOH (20:1) yielding **3** (0.15 g, 61% yield). 1H NMR (400 MHz, $CDCl_3$) δ 7.55–7.18 (m, 15H), 3.12–3.01 (m, 1H), 2.17–1.98 (m, 1H), 1.96–1.83 (m, 1H), 1.81–1.56 (m, 2H), 1.41 (s, 9H). ^{13}C NMR (101 MHz, $CDCl_3$) δ 177.8, 171.1, 142.2, 141.0, 129.0, 127.8, 82.3, 81.4, 56.0, 29.3, 28.0, 24.9.

4.7.5. *Tert*-butyl 2-(4-(((2-amino-4-oxo-3,4-dihydropteridin-6-yl)methyl)amino)benzamido)-5-oxo-5-((trityloxy)amino)pentanoate (**5**): representative procedure for amide bond formation from acyl azide and amine

Pteroyl azide (0.13 g, 0.40 mmol) and **3** (0.14 g, 0.30 mmol) were dissolved in DMSO. Upon addition of tetramethylguanidine (0.07 g,

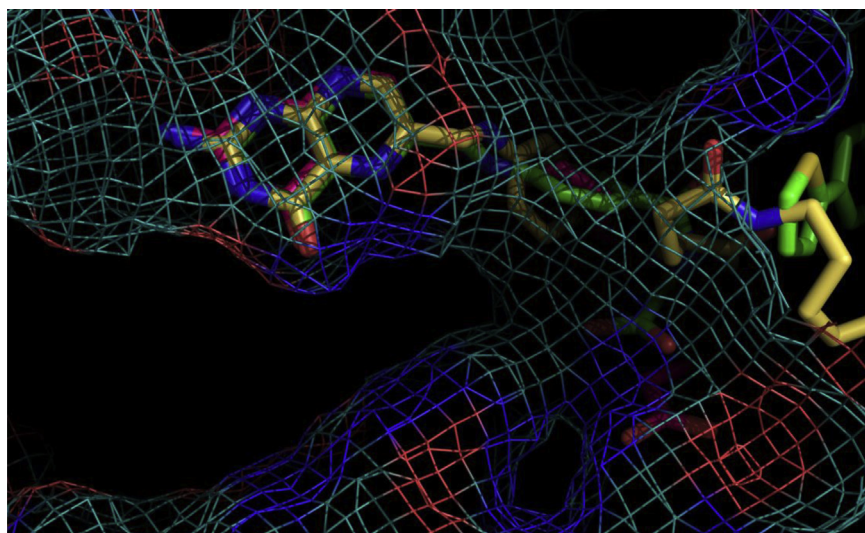


Fig. 12. Molecular docking of the FR (PDB code: 4LRH) with folic acid (pink), **24b** (gold) and **24c** (green) showing similar binding mode between their pterin moiety and FR binding pocket. (For interpretation of the references to color in this figure legend, the reader is referred to the web version of this article.)

0.61 mmol), the reaction was stirred overnight at room temperature. Dropwise addition of acetonitrile resulted in a yellow precipitate which was collected by centrifugation and washed by Et₂O. The crude product was purified by preparative TLC with Et₂O:N-H₄OH:Isopropanol:EtOH (2:1:1:1) to yield a yellow powder **5** (0.048 g, 21%). ¹H NMR (400 MHz, DMSO-*d*₆) δ 8.62 (s, 1H), 7.59 (d, *J* = 8.4 Hz, 2H), 7.29 (s, 15H), 6.60 (d, *J* = 7.5 Hz, 2H), 4.47 (s, 2H), 4.20–3.87 (m, 1H), 1.98–1.77 (m, 2H), 1.74–1.49 (m, 2H), 1.34 (s, 9H). ¹³C NMR (101 MHz, DMSO-*d*₆) δ 171.8, 166.8, 154.3, 151.2, 149.0, 142.8, 129.4, 128.4, 128.0, 121.7, 111.6, 92.3, 80.7, 56.3, 53.2, 46.3, 28.1.

4.7.6. 2-(4-(((2-Amino-4-oxo-3,4-dihydropteridin-6-yl)methyl)amino)benzamido)-5-(hydroxyamino)-5-oxopentanoic acid (**6**): representative procedure for protecting groups removal

Compound **5** (0.046 g, 0.061 mmol) was dissolved in neat TFA (2 mL) containing TIPS (0.5 mL) and stirred at room temperature for 2 h. The slurry residue obtained upon the TFA evaporation was added to acetonitrile dropwise resulting in a precipitate which was collected by centrifugation. The precipitate was washed with Et₂O (4 × 40 mL) and dried yielding a yellow powder **6** (0.028 g, quantitative yield). ¹H NMR (400 MHz, DMSO-*d*₆) δ 8.67 (s, 1H), 7.60 (d, *J* = 8.6 Hz, 2H), 6.61 (d, *J* = 8.5 Hz, 2H), 4.51 (s, 2H), 4.27–4.17 (m, 1H), 2.12–1.96 (m, 3H), 1.95–1.83 (m, 1H). ¹³C NMR (126 MHz, DMSO-*d*₆) δ 174.2, 174.0, 168.9, 166.7, 151.1, 148.9, 129.3, 128.2, 121.6, 111.5, 52.4, 30.7, 29.3. HRMS (ESI) calcd for C₁₉H₂₁N₈O₆ [M+H]⁺ 457.1579 found 457.1567.

4.7.7. 4-(((2-Amino-4-oxo-3,4-dihydropteridin-6-yl)methyl)amino)-*N*-hydroxybenzamide (**7**)

An intermediate in the synthesis of pteroyl azide, N₁₀-(trifluoroacetyl)pyrofolinic acid (0.25 g), was dissolved in DMSO (6 mL) followed by the addition of a 50% aqueous hydroxylamine solution (0.15 mL). After stirring at room temperature for 5 h, the reaction was added dropwise to acetonitrile. The yellow precipitate thus obtained was collected by centrifugation and washed with Et₂O (4 × 40 mL), MeOH (2 × 30 mL) and dried. Multiple rounds of DMSO dissolution and precipitation were conducted to obtain the desired purity of **7**, a dark yellow precipitate (0.050 g, 32% yield). ¹H NMR (400 MHz, DMSO-*d*₆) δ 8.62 (s, 1H), 7.49 (d, *J* = 8.7 Hz, 2H), 6.59 (d, *J* = 8.8 Hz, 2H), 4.44 (d, *J* = 6.2 Hz, 2H). ¹³C NMR (126 MHz, DMSO-*d*₆) δ 167.7, 165.1, 154.1, 152.2, 150.9, 148.9, 131.4, 128.6, 128.2, 120.3, 118.4, 111.6, 46.2. HRMS (ESI) calcd for C₁₄H₁₄N₇O₃ [M+H]⁺ 328.1153 found 328.1160.

4.7.7.1. 4-Amino-*N*-(trityloxy)butanamide (**9a**): representative procedure of azide reduction with PPh₃. Trityl protected hydroxamate azide **8a** (1.5 g, 3.88 mmol) and PPh₃ (2.44 g, 9.32 mmol) were dissolved in anhydrous THF (6 mL) and stirred at room temperature under inert atmosphere overnight. H₂O was then added and the reaction allowed to proceed at room temperature for 2 h. DCM was added to the reaction and washed with H₂O (3 × 50 mL), brine (50 mL) and dried with Na₂SO₄. The crude product was purified by column chromatography eluted with DCM:MeOH:NH₄OH (10:1:0.1) to yield **9a** (0.91 g, 65% yield). ¹H NMR (400 MHz, DMSO-*d*₆) δ 7.29 (dd, *J* = 13.7, 4.6 Hz, 15H), 2.29 (t, *J* = 6.4 Hz, 2H), 1.81 (t, *J* = 7.0 Hz, 2H), 1.36–1.22 (m, 2H). ¹³C NMR (101 MHz, CDCl₃) δ 174.7, 146.0, 144.9, 133.0, 132.0, 131.6, 131.5, 96.9, 44.2, 34.0, 31.4.

4.7.7.2. 5-Amino-*N*-(trityloxy)pentanamide (**9b**). Compound **8b** (1.5 g, 3.75 mmol) was reacted with PPh₃ (2.36 g, 8.99 mmol) in THF as described for the synthesis of **9a** to give **9b** (0.8 g, 57% yield). ¹H NMR (400 MHz, DMSO-*d*₆) δ 7.28 (dd, *J* = 10.3, 3.6 Hz, 15H), 2.35 (t, *J* = 7.0 Hz, 2H), 1.74 (t, *J* = 7.3 Hz, 2H), 1.26–1.15 (m, 2H), 1.09–1.00 (m, 2H). ¹³C NMR (101 MHz, CDCl₃) δ 141.8, 140.8, 129.0, 128.2, 127.8,

93.2, 38.9, 31.5, 30.2, 26.3.

4.7.7.3. 6-Amino-*N*-(trityloxy)hexanamide (**9c**). Compound **8c** (0.5 g, 1.21 mmol) was reacted with PPh₃ (0.76 g, 1.9 mmol) in THF as described for the synthesis of **9a** to give **9c** (0.34 g, 72% yield). ¹H NMR (500 MHz, CDCl₃) δ 7.64–7.21 (m, 15H), 2.61 (t, *J* = 6.2 Hz, 2H), 1.95–1.82 (m, 1H), 1.69–1.53 (m, 1H), 1.49–0.96 (m, 6H). ¹³C NMR (126 MHz, CDCl₃) δ 177.0, 141.9, 140.9, 128.9, 128.0, 127.8, 127.5, 93.2, 50.1, 41.5, 32.7, 31, 26.1, 24.6, 23.

4.7.7.4. 7-Amino-*N*-(trityloxy)heptanamide (**9d**). Compound **8d** (1.5 g, 3.5 mmol) was reacted with PPh₃ (2.2 g, 8.4 mmol) in THF as described for the synthesis of **9a** to give **9d** (1.25 g, 89% yield). ¹H NMR (400 MHz, DMSO-*d*₆) δ 7.30 (s, 15H), 2.43 (t, *J* = 6.8 Hz, 2H), 1.75 (t, *J* = 7.0 Hz, 2H), 1.27–1.02 (m, 6H), 0.98–0.87 (m, 2H). ¹³C NMR (101 MHz, DMSO-*d*₆) δ 170.7, 142.9, 129.4, 127.9, 127.8, 92.1, 41.9, 33.3, 32.4, 28.7, 26.5, 25.3.

4.7.7.5. 8-Amino-*N*-(trityloxy)octanamide (**9e**). Compound **8e** (1.5 g, 3.39 mmol) was reacted with PPh₃ (2.13 g, 8.13 mmol) in THF as described for the synthesis of **9a** to give **9e** (1.16 g, 82% yield). ¹H NMR (400 MHz, DMSO-*d*₆) δ 7.38–7.15 (m, 15H), 2.46 (t, *J* = 5.3 Hz, 2H), 1.75 (t, *J* = 7.2 Hz, 2H), 1.32–1.21 (m, 2H), 1.20–1.01 (m, 6H), 0.99–0.88 (m, 2H). ¹³C NMR (101 MHz, DMSO-*d*₆) δ 170.6, 143.0, 129.4, 128, 127.8, 92.1, 55.4, 42.0, 33.6, 29.1, 28.8, 26.7, 25.2.

4.7.7.6. 9-Amino-*N*-(trityloxy)nonanamide (**9f**). Compound **8f** (0.98 g, 2.15 mmol) was reacted with PPh₃ (1.35 g, 5.15 mmol) in THF as described for the synthesis of **9a** to give **9f** (0.8 g, 86% yield). ¹H NMR (400 MHz, CDCl₃) δ 7.56–7.21 (m, 15H), 2.65 (t, *J* = 7.0 Hz, 2H), 1.65–1.50 (m, 2H), 1.48–1.36 (m, 2H), 1.31–0.98 (m, 10H). ¹³C NMR (101 MHz, CDCl₃) δ 177.4, 141.1, 129.0, 128.1, 128.1, 105.0, 93.3, 53.4, 42.0, 33.5, 29.2, 29.0, 26.8, 23.5.

4.7.7.7. 10-Amino-*N*-(trityloxy)decanamide (**9g**). Compound **8g** (1.5 g, 3.19 mmol) was reacted with PPh₃ (2.0 g, 7.65 mmol) in THF as described for the synthesis of **9a** to give **9g** (1.22 g, 86% yield). ¹H NMR (400 MHz, CDCl₃) δ 7.63–7.13 (m, 15H), 2.71 (t, *J* = 6.8 Hz, 2H), 2.01–1.70 (m, 2H), 1.57–1.47 (m, 2H), 1.33–0.93 (m, 12H). ¹³C NMR (101 MHz, CDCl₃) δ 177.4, 141.1, 129.0, 128.8, 128.1, 127.8, 105.0, 93.3, 41.2, 31.2, 30.9, 29.2, 29.1, 26.7, 23.4.

4.7.7.8. 4-(((2-Amino-4-oxo-3,4-dihydropteridin-6-yl)methyl)amino)-*N*-(4-oxo-4-((trityloxy)amino)butyl)benzamide (**10a**). Compound **9a** (0.2 g, 0.55 mmol) was coupled to pteroyl azide (0.24 g, 0.72 mmol) in the presence of TMG (0.13 g, 1.11 mmol) in DMSO as described for the synthesis of **5** to yield **10a** (0.11 g, 31% yield). ¹H NMR (400 MHz, DMSO-*d*₆) δ 8.62 (s, 1H), 7.54 (d, *J* = 8.5 Hz, 2H), 7.29 (s, 15H), 6.59 (d, *J* = 8.6 Hz, 2H), 4.45 (d, *J* = 5.8 Hz, 2H), 2.98 (dd, *J* = 12.5, 7.1 Hz, 2H), 1.77 (t, *J* = 7.5 Hz, 2H), 1.39 (t, *J* = 8.1 Hz, 2H). ¹³C NMR (101 MHz, DMSO-*d*₆) δ 166.6, 161.8, 154.4, 150.9, 149.0, 142.8, 129.3, 129.1, 128.0, 127.9, 111.7, 92.2, 65.4, 56.5, 46.3, 18.9, 15.6.

4.7.7.9. 4-(((2-Amino-4-oxo-3,4-dihydropteridin-6-yl)methyl)amino)-*N*-(4-(hydroxyamino)-4-oxobutyl)benzamide (**10b**). Compound **9b** (0.2 g, 0.53 mmol) was coupled to pteroyl azide (0.23 g, 0.69 mmol) in the presence of TMG (0.12 g, 1.07 mmol) in DMSO as described for the synthesis of **5** to yield **10b** (0.12 g, 33% yield). ¹H NMR (400 MHz, DMSO-*d*₆) δ 8.62 (s, 1H), 7.57 (d, *J* = 8.0 Hz, 2H), 7.29 (s, 14H), 6.60 (d, *J* = 8.0 Hz, 2H), 4.45 (d, *J* = 5.9 Hz, 2H), 3.09–2.93 (m, 2H), 1.90–1.69 (m, 2H), 1.30–1.02 (m, 4H). ¹³C NMR (101 MHz, DMSO-*d*₆) δ 166.4, 154.3, 150.9, 149.0, 142.9, 129.4, 129.0, 128.4, 127.9, 127.8, 122.6, 111.6, 92.1, 46.4, 29.1, 22.8.

4.7.7.10. 4-(((2-Amino-4-oxo-3,4-dihydropteridin-6-yl)methyl)amino)-N-(6-oxo-6-((trityloxy)amino)hexyl)benzamide (**10c**).

Compound **9c** (0.2 g, 0.52 mmol) was coupled to pteroyl azide (0.26 g, 0.77 mmol) in the presence of TMG (0.12 g, 1.03 mmol) in DMSO as described for the synthesis of **5** to yield **10c** (0.10 g, 29% yield). ¹H NMR (400 MHz, DMSO-*d*₆) δ 8.62 (s, 1H), 7.57 (d, *J* = 8.3 Hz, 2H), 7.30 (s, 14H), 6.59 (d, *J* = 8.1 Hz, 2H), 4.45 (d, *J* = 5.7 Hz, 2H), 3.07 (dd, *J* = 11.6, 6.0 Hz, 2H), 1.74 (t, *J* = 11.6 Hz, 2H), 1.38–1.11 (m, 4H), 1.04–0.88 (m, 2H). ¹³C NMR (101 MHz, DMSO-*d*₆) δ 166.4, 154.3, 150.9, 149.0, 142.9, 129.4, 129.0, 127.9, 122.6, 111.6, 105.0, 92.2, 46.4, 32.4, 29.5, 26.4, 25.0.

4.7.7.11. 4-(((2-Amino-4-oxo-3,4-dihydropteridin-6-yl)methyl)amino)-N-(7-oxo-7-((trityloxy)amino)heptyl)benzamide (**10d**).

Compound **9d** (0.2 g, 0.5 mmol) was coupled to pteroyl azide (0.22 g, 0.65 mmol) in the presence of TMG (0.11 g, 0.99 mmol) in DMSO as described for the synthesis of **5** to yield **10d** (0.14 g, 41% yield). ¹H NMR (400 MHz, DMSO-*d*₆) δ 8.61 (s, 1H), 7.56 (d, *J* = 8.1 Hz, 2H), 7.29 (s, 16H), 6.58 (d, *J* = 8.8 Hz, 2H), 4.44 (d, *J* = 5.2 Hz, 2H), 3.13–3.03 (m, 2H), 1.80–1.68 (m, 2H), 1.41–1.28 (m, 2H), 1.20–1.04 (m, 4H), 1.00–0.87 (m, 2H). ¹³C NMR (101 MHz, DMSO-*d*₆) δ 172.7, 166.4, 154.3, 150.9, 149.9, 149.0, 129.4, 129.0, 127.9, 127.8, 122.6, 111.6, 92.1, 55.4, 29.6, 26.6.

4.7.7.12. 4-(((2-Amino-4-oxo-3,4-dihydropteridin-6-yl)methyl)amino)-N-(8-oxo-8-((trityloxy)amino)octyl)benzamide (**10e**).

Compound **9e** (0.2 g, 0.48 mmol) was coupled to pteroyl azide (0.21 g, 0.62 mmol) in the presence of TMG (0.11 g, 0.96 mmol) in DMSO as described for the synthesis of **5** to yield **10e** (0.15 g, 45% yield). ¹H NMR (400 MHz, DMSO-*d*₆) δ 8.61 (s, 1H), 7.57 (d, *J* = 8.5 Hz, 2H), 7.29 (s, 15H), 6.59 (d, *J* = 8.5 Hz, 2H), 4.44 (d, *J* = 5.9 Hz, 2H), 3.13 (d, *J* = 6.0 Hz, 2H), 1.73 (t, *J* = 7.5 Hz, 2H), 1.44–1.32 (m, 2H), 1.24–1.08 (m, 6H), 0.97–0.87 (m, 2H). ¹³C NMR (101 MHz, DMSO-*d*₆) δ 166.4, 154.3, 150.9, 149.0, 142.9, 129.4, 129.0, 127.9, 122.6, 111.6, 92.1, 65.4, 46.4, 29.8, 28.9, 26.8, 25.2, 15.6.

4.7.7.13. 4-(((2-Amino-4-oxo-3,4-dihydropteridin-6-yl)methyl)amino)-N-(9-oxo-9-((trityloxy)amino)nonyl)benzamide (**10f**).

Compound **9f** (0.2 g, 0.46 mmol) was coupled to pteroyl azide (0.20 g, 0.60 mmol) in the presence of TMG (0.11 g, 0.93 mmol) in DMSO as described for the synthesis of **5** to yield **10f** (0.088 g, 26% yield). ¹H NMR (400 MHz, DMSO-*d*₆) δ 8.62 (s, 1H), 7.58 (d, *J* = 8.6 Hz, 2H), 7.30 (s, 15H), 6.60 (d, *J* = 8.7 Hz, 2H), 4.45 (d, *J* = 5.8 Hz, 2H), 3.19–3.10 (m, 2H), 1.74 (t, *J* = 7.8 Hz, 2H), 1.42 (t, *J* = 8.5 Hz, 2H), 1.22–1.00 (m, 8H), 0.99–0.88 (m, 2H). ¹³C NMR (101 MHz, DMSO-*d*₆) δ 166.4, 154.3, 150.9, 149.0, 142.9, 129.4, 129.0, 128.4, 127.9, 127.8, 122.6, 111.6, 106.0, 96.3, 46.4, 29.8, 29.1, 26.9.

4.7.7.14. 4-(((2-Amino-4-oxo-3,4-dihydropteridin-6-yl)methyl)amino)-N-(10-oxo-10-((trityloxy)amino)decyl)benzamide (**10g**).

Compound **9g** (0.2 g, 0.45 mmol) was coupled to pteroyl azide (0.2 g, 0.59 mmol) in the presence of TMG (0.10 g, 0.89 mmol) in DMSO as described for the synthesis of **5** to yield **10g** (0.15 g, 45% yield). ¹H NMR (400 MHz, DMSO-*d*₆) δ 8.62 (s, 1H), 7.57 (d, *J* = 8.8 Hz, 2H), 7.30 (s, 15H), 6.59 (d, *J* = 8.8 Hz, 2H), 4.44 (d, *J* = 5.9 Hz, 2H), 3.14 (dd, *J* = 12.8, 6.4 Hz, 2H), 1.74 (t, *J* = 7.9 Hz, 2H), 1.48–1.35 (m, 2H), 1.26–1.04 (m, 10H), 0.98–0.87 (m, 2H). ¹³C NMR (101 MHz, DMSO-*d*₆) δ 166.4, 154.3, 150.9, 149.0, 142.9, 129.4, 129.0, 127.9, 127.8, 122.7, 122.0, 111.6, 85.9, 46.4, 29.8, 29.3, 29.2, 29.1, 28.8, 28.7, 27.0.

4.7.7.15. 4-(((2-Amino-4-oxo-3,4-dihydropteridin-6-yl)methyl)amino)-N-(4-(hydroxyamino)-4-oxobutyl)benzamide (**11a**).

Compound **10a** (0.099 g, 0.15 mmol) was dissolved in neat TFA (2 mL) and TIPS (0.5 mL) and stirred at room temperature for 2 h.

The desired product **11a** (0.05 g, 81% yield) was obtained as described for the synthesis of **6**. ¹H NMR (500 MHz, DMSO-*d*₆) δ 8.65 (s, 1H), 7.61 (d, *J* = 8.0 Hz, 2H), 6.63 (d, *J* = 8.0 Hz, 2H), 4.48 (d, *J* = 5.3 Hz, 2H), 3.24–3.13 (m, 2H), 1.98 (t, *J* = 7.2 Hz, 2H), 1.81–1.59 (m, 2H). ¹³C NMR (126 MHz, DMSO-*d*₆) δ 174.42, 169.2, 166.4, 161.1, 156.9, 154.0, 150.8, 149.0, 128.9, 128.2, 122.3, 111.5, 46.2, 33.0, 30.3, 25.8, 25.6. HRMS (ESI) calcd for C₁₈H₂₁N₈O₄ [M+H]⁺ 413.1680 found 413.1692.

4.7.7.16. 4-(((2-Amino-4-oxo-3,4-dihydropteridin-6-yl)methyl)amino)-N-(5-(hydroxyamino)-5-oxopentyl)benzamide (**11b**).

Compound **10b** (0.054 g, 0.081 mmol) was dissolved in neat TFA (2 mL) and TIPS (0.5 mL) and stirred at room temperature for 2 h. The desired product **11b** (0.025 g, 72% yield) was obtained as described for the synthesis of **6**. ¹H NMR (400 MHz, DMSO-*d*₆) δ 8.61 (s, 1H), 7.57 (d, *J* = 7.4 Hz, 2H), 6.59 (d, *J* = 7.4 Hz, 2H), 4.43 (s, 2H), 3.20–3.04 (m, 2H), 1.92 (t, *J* = 6.3 Hz, 2H), 1.56–1.30 (m, 4H). ¹³C NMR (126 MHz, DMSO-*d*₆) δ 169.3, 166.3, 154.0, 150.7, 148.9, 128.9, 128.2, 122.4, 111.5, 46.2, 32.3, 29.3, 23.0. HRMS (ESI) calcd for C₁₉H₂₃N₈O₄ [M+H]⁺ 427.1837 found 427.1845.

4.7.7.17. 4-(((2-Amino-4-oxo-3,4-dihydropteridin-6-yl)methyl)amino)-N-(6-(hydroxyamino)-6-oxohexyl)benzamide (**11c**).

Compound **10c** (0.081 g, 0.12 mmol) was dissolved in neat TFA (2 mL) and TIPS (0.5 mL) and stirred at room temperature for 2 h. The desired product **11c** (0.048 g, 92% yield) was obtained as described for the synthesis of **6**. ¹H NMR (400 MHz, DMSO-*d*₆) δ 8.62 (s, 1H), 7.57 (d, *J* = 7.0 Hz, 2H), 6.59 (d, *J* = 7.2 Hz, 2H), 4.44 (s, 2H), 3.15–3.05 (m, 2H), 1.90 (t, *J* = 7.2 Hz, 2H), 1.54–1.33 (m, 4H), 1.33–1.12 (m, 2H). ¹³C NMR (126 MHz, DMSO-*d*₆) δ 169.4, 166.2, 161.2, 154.0, 150.7, 148.9, 128.9, 128.2, 122.5, 111.5, 46.2, 32.5, 29.4, 26.4, 25.2. HRMS (ESI) calcd for C₂₀H₂₅N₈O₄ [M+H]⁺ 441.1993 found 441.1977.

4.7.7.18. 4-(((2-Amino-4-oxo-3,4-dihydropteridin-6-yl)methyl)amino)-N-(7-(hydroxyamino)-7-oxoheptyl)benzamide (**11d**).

Compound **10d** (0.12 g, 0.17 mmol) was dissolved in neat TFA (2 mL) and TIPS (0.5 mL) and stirred at room temperature for 2 h. The desired product **11d** (0.066 g, 85% yield) was obtained as described for the synthesis of **6**. ¹H NMR (500 MHz, DMSO-*d*₆) δ 8.65 (s, 1H), 7.60 (d, *J* = 8.5 Hz, 2H), 6.62 (d, *J* = 8.6 Hz, 2H), 4.48 (d, *J* = 5.8 Hz, 2H), 3.17 (dd, *J* = 12.7, 6.4 Hz, 2H), 1.93 (t, *J* = 7.3 Hz, 2H), 1.53–1.40 (m, 4H), 1.26 (d, *J* = 2.8 Hz, 4H). ¹³C NMR (126 MHz, DMSO-*d*₆) δ 169.4, 166.3, 154.0, 150.7, 149.0, 128.9, 128.2, 122.5, 111.5, 46.2, 32.5, 29.5, 28.7, 26.5, 25.4. HRMS (ESI) calcd for C₂₁H₂₇N₈O₄ [M+H]⁺ 455.2150 found 455.2137.

4.7.7.19. 4-(((2-Amino-4-oxo-3,4-dihydropteridin-6-yl)methyl)amino)-N-(8-(hydroxyamino)-8-oxooctyl)benzamide (**11e**).

Compound **10e** (0.13 g, 0.18 mmol) was dissolved in neat TFA (2 mL) and TIPS (0.5 mL) and stirred at room temperature for 2 h. The desired product **11e** (0.082 g, 97% yield) was obtained as described for the synthesis of **6**. ¹H NMR (500 MHz, DMSO-*d*₆) δ 8.65 (s, 1H), 7.60 (d, *J* = 8.0 Hz, 2H), 6.62 (d, *J* = 8.0 Hz, 2H), 4.48 (d, *J* = 4.4 Hz, 2H), 3.21–3.12 (m, 2H), 1.92 (t, *J* = 14.3 Hz, 2H), 1.55–1.39 (m, 4H), 1.33–1.16 (m, 6H). ¹³C NMR (126 MHz, DMSO-*d*₆) δ 169.4, 166.3, 154.0, 150.7, 149.0, 128.9, 128.2, 122.5, 112.8, 111.5, 55.2, 46.2, 32.5, 29.6, 28.8, 28.8, 26.7, 25.4. HRMS (ESI) calcd for C₂₂H₂₉N₈O₄ [M+H]⁺ 469.2306 found 469.2290.

4.7.7.20. 4-(((2-Amino-4-oxo-3,4-dihydropteridin-6-yl)methyl)amino)-N-(9-(hydroxyamino)-9-oxononyl)benzamide (**11f**).

Compound **10f** (0.053 g, 0.073 mmol) was dissolved in neat TFA (2 mL) and TIPS (0.5 mL) and stirred at room temperature for 2 h. The desired product **11f** (0.024 g, 70% yield) was obtained as

described for the synthesis of **6**. ^1H NMR (400 MHz, DMSO- d_6) δ 8.71 (s, 1H), 7.57 (d, J = 6.4 Hz, 2H), 6.60 (d, J = 8.0 Hz, 2H), 4.53 (s, 2H), 3.14 (t, J = 11.7 Hz, 2H), 1.89 (t, J = 8.4 Hz, 2H), 1.52–1.34 (m, 4H), 1.29–1.06 (m, 10H). HRMS (ESI) calcd for $\text{C}_{23}\text{H}_{31}\text{N}_8\text{O}_4$ [$\text{M}+\text{H}$] $^+$ 483.2463 found 483.2452.

4.7.7.21. 4-(((2-Amino-4-oxo-3,4-dihydropteridin-6-yl)methyl)amino)-N-(10-(hydroxyamino)-10-oxodecyl)benzamide (**11g**). Compound **10g** (0.13 g, 0.17 mmol) was dissolved in neat TFA (2 mL) and TIPS (0.5 mL) and stirred at room temperature for 2 h. The desired product **11g** (0.075 g, 89% yield) was obtained as described for the synthesis of **6**. ^1H NMR (400 MHz, DMSO- d_6) δ 8.66 (s, 1H), 7.56 (d, J = 8.5 Hz, 2H), 6.58 (d, J = 7.8 Hz, 2H), 4.48 (s, 2H), 3.21–3.05 (m, 2H), 1.89 (t, J = 6.5 Hz, 2H), 1.54–1.37 (m, 4H), 1.21 (dd, J = 14.9, 5.8 Hz, 10H). ^{13}C NMR (126 MHz, DMSO- d_6) δ 175.5, 167.2, 160.1, 152.8, 130.3, 128.8, 114.0, 66.5, 39.8, 33.8, 29.2, 28.9, 28.8, 28.7, 28.6, 26.5, 25.2, 24.6. HRMS (ESI) calcd for $\text{C}_{26}\text{H}_{25}\text{N}_8\text{O}_3$ [$\text{M}+\text{H}$] $^+$ 497.2044 found 497.2060.

4.7.7.22. (*S*)-*Tert*-butyl 2-azido-5-oxo-5-((4-oxo-4-((trityloxy)amino)butyl)amino)pentanoate (**12a**): representative protocol for amide synthesis with EDCl. The α -azido *L*-glutamic acid α -*tert*-butyl ester **1** (0.27 g, 1.17 mmol), EDCl (0.22 g, 1.17 mmol) and HOBT (0.16 g, 1.17 mmol) were dissolved in DMF and stirred at room temperature for 30 min. The *O*-trityl protected hydroxamate **9a** (0.3 g, 0.83 mmol) was added and the mixture allowed to stir overnight at room temperature. DCM was added to the reaction and then washed with H_2O (3 \times 50 mL), NaHCO_3 (1 \times 50 mL), brine (1 \times 50 mL) and dried with Na_2SO_4 . The crude product was purified by preparative TLC using EtOAc:Hexanes (1:1) to yield **12a** (0.23 g, 45% yield). ^1H NMR (400 MHz, CDCl_3) δ 7.54–7.20 (m, 15H), 3.87–3.70 (m, 1H), 3.12–2.99 (m, 1H), 2.96–2.85 (m, 1H), 2.28–2.05 (m, 3H), 2.00–1.81 (m, 2H), 1.70–1.54 (m, 2H), 1.53–1.35 (m, 10H). ^{13}C NMR (101 MHz, CDCl_3) δ 169.2, 141.9, 140.9, 129.0, 128.2, 127.8, 93.6, 83.0, 61.8, 39.3, 32.1, 29.2, 28.0, 27.0, 22.5.

4.7.7.23. (*S*)-*Tert*-butyl 2-azido-5-oxo-5-((7-oxo-7-((trityloxy)amino)heptyl)amino)pentanoate (**12b**). The α -azido *L*-glutamic acid α -*tert*-butyl ester **1** (0.2 g, 0.87 mmol) was coupled to **9d** (0.35 g, 0.87 mmol) in the presence of IBCF (0.12 g, 0.87 mmol) and NMM (0.27 g, 2.62 mmol) as described for the synthesis of **2**. Purification of the crude product was done by prep TLC in EtOAc:Hexanes (1:1) resulting in **12b** (0.33 g, 61% yield). ^1H NMR (400 MHz, CDCl_3) δ 7.53–7.12 (m, 15H), 3.78 (dd, J = 9.0, 4.8 Hz, 1H), 3.20–3.04 (m, 2H), 2.28–2.19 (m, 2H), 2.19–2.08 (m, 1H), 1.93 (dt, J = 13.8, 10.5 Hz, 1H), 1.85–1.76 (m, 1H), 1.62–1.51 (m, 1H), 1.46 (s, 9H), 1.42–1.29 (m, 3H), 1.28–0.92 (m, 5H). ^{13}C NMR (101 MHz, CDCl_3) δ 177.3, 171.4, 169.2, 141.9, 141.1, 129.0, 128.1, 127.8, 93.4, 83.0, 61.8, 39.4, 32.1, 31.1, 29.2, 28.6, 28.0, 27.1, 26.5, 23.2.

4.7.7.24. (*S*)-*Tert*-butyl 2-azido-5-oxo-5-((8-oxo-8-((trityloxy)amino)octyl)amino)pentanoate (**12c**). The α -azido *L*-glutamic acid α -*tert*-butyl ester **1** (0.19 g, 0.83 mmol) was coupled to **9e** (0.45 g, 1.08 mmol) in the presence of IBCF (0.11 g, 0.83 mmol) and NMM (0.25 g, 2.49 mmol) as described for the synthesis of **2**. Purification of the crude product was done by prep TLC in EtOAc:Hexanes (1:1) resulting in **12c** (0.28 g, 54% yield). ^1H NMR (500 MHz, CDCl_3) δ 7.43 (d, J = 65.5 Hz, 15H), 3.85 (dd, J = 8.9, 4.9 Hz, 1H), 3.28–3.16 (m, 2H), 2.30 (t, J = 7.2 Hz, 2H), 2.21 (dt, J = 13.5, 7.0 Hz, 1H), 1.99 (dq, J = 14.2, 7.0 Hz, 1H), 1.92–1.82 (m, 1H), 1.66–1.56 (m, 1H), 1.52 (s, 9H), 1.49–1.42 (m, 2H), 1.31–0.99 (m, 8H). ^{13}C NMR (126 MHz, CDCl_3) δ 171.1, 169.1, 128.9, 128.0, 82.9, 61.6, 39.4, 32.0, 29.2, 28.6, 27.8, 26.9, 26.3.

4.7.7.25. (*S*)-*Tert*-butyl 2-azido-5-oxo-5-((9-oxo-9-((trityloxy)amino)nonyl)amino)pentanoate (**12d**). The α -azido *L*-glutamic acid α -*tert*-butyl ester **1** (0.2 g, 0.87 mmol) was coupled to **9f** (0.38 g, 0.87 mmol) in the presence of IBCF (0.12 g, 0.87 mmol) and NMM (0.27 g, 2.62 mmol) as described for the synthesis of **2**. Purification of the crude product was done by prep TLC in EtOAc:Hexanes (1:1) resulting in **12d** (0.34 g, 60% yield). ^1H NMR (500 MHz, CDCl_3) δ 7.59–7.27 (m, 15H), 3.89 (ddd, J = 42.9, 8.9, 4.8 Hz, 1H), 3.31–3.12 (m, 2H), 2.29 (t, J = 7.1 Hz, 2H), 2.25–2.16 (m, 1H), 1.99 (dq, J = 14.3, 7.0 Hz, 1H), 1.93–1.79 (m, 1H), 1.60 (t, J = 20.4 Hz, 1H), 1.52 (s, 9H), 1.50–1.43 (m, 2H), 1.33–0.99 (m, 10H). ^{13}C NMR (126 MHz, CDCl_3) δ 171.0, 169.1, 140.9, 128.9, 128.0, 82.9, 61.6, 39.4, 32.0, 29.4, 28.7, 27.9, 26.9, 26.5.

4.7.7.26. (*S*)-*Tert*-butyl 2-amino-5-oxo-5-((4-oxo-4-((trityloxy)amino)butyl)amino)pentanoate (**13a**). To a solution of **12a** (0.22 g, 0.39 mmol) in EtOH (6 mL) and H_2O (2 mL), NH_4Cl (0.094 g, 1.76 mmol) and zinc powder (0.12 g) were added and the resulting mixture was stirred under reflux for 2 h. After completion of the reaction, the mixture was filtered through a celite pad. Following the removal of the solvent, the crude product was purified by preparative TLC with DCM:MeOH: NH_4OH (10:1:0.1) yielding **13a** (0.097 g, 46% yield). ^1H NMR (400 MHz, CDCl_3) δ 7.51–7.19 (m, 15H), 3.24 (s, 1H), 3.09–2.84 (m, 2H), 2.21 (t, J = 7.4 Hz, 2H), 2.06–1.93 (m, 1H), 1.90–1.82 (m, 1H), 1.76–1.66 (m, 1H), 1.64–1.54 (m, 2H), 1.43 (s, 9H), 1.40–1.36 (m, 1H). ^{13}C NMR (101 MHz, CDCl_3) δ 176.9, 142.1, 140.9, 129.1, 128.1, 127.8, 127.6, 93.5, 81.2, 54.4, 39.2, 32.8, 30.4, 29.0, 28.0, 22.8.

4.7.7.27. (*S*)-*Tert*-butyl 2-amino-5-oxo-5-((7-oxo-7-((trityloxy)amino)heptyl)amino)pentanoate (**13b**). Compound **12b** (0.28 g, 0.45 mmol) was reduced in the presence of NH_4Cl (0.058 g, 1.08 mmol) and zinc powder (0.042 g) as described for **13a**. Prep TLC with DCM:MeOH: NH_4OH (10:1:0.1) yielded **13b** (0.25 g, 93% yield). ^1H NMR (400 MHz, CDCl_3) δ 7.52–7.10 (m, 15H), 3.59–3.40 (m, 1H), 3.21–3.01 (m, 2H), 2.43–2.24 (m, 2H), 2.21–2.06 (m, 1H), 1.96–1.77 (m, 2H), 1.62–1.52 (m, 1H), 1.44 (s, 9H), 1.40–1.34 (m, 3H), 1.23–1.05 (m, 5H). ^{13}C NMR (101 MHz, CDCl_3) δ 177.3, 172.2, 142.0, 141.1, 129.0, 128.1, 127.9, 127.8, 127.7, 93.3, 82.2, 54.0, 39.4, 32.6, 31.1, 29.1, 28.6, 28.0, 26.5, 24.9, 23.2.

4.7.7.28. (*S*)-*Tert*-butyl 2-amino-5-oxo-5-((8-oxo-8-((trityloxy)amino)octyl)amino)pentanoate (**13c**). Compound **12c** (0.25 g, 0.39 mmol) was reduced in the presence of NH_4Cl (0.05 g, 0.94 mmol) and zinc powder (0.036 g) as described for **13a**. Prep TLC with DCM:MeOH: NH_4OH (10:1:0.1) yielded **13c** (0.20 g, 85% yield). ^1H NMR (400 MHz, CDCl_3) δ 7.58–7.11 (m, 15H), 3.37–3.24 (m, 1H), 3.16 (dd, J = 12.7, 6.4 Hz, 2H), 2.28 (t, J = 7.4 Hz, 2H), 2.11–2.01 (m, 1H), 1.87–1.69 (m, 2H), 1.61–1.51 (m, 1H), 1.48–1.34 (m, 10H), 1.33–0.94 (m, 8H). ^{13}C NMR (101 MHz, CDCl_3) δ 177.3, 174.7, 172.3, 141.9, 141.1, 129.0, 128.1, 127.9, 93.3, 81.4, 54.3, 39.4, 33.0, 31.1, 30.3, 29.7, 29.4, 28.8, 28.0, 26.6, 23.2.

4.7.7.29. (*S*)-*Tert*-butyl 2-amino-5-oxo-5-((9-oxo-9-((trityloxy)amino)nonyl)amino)pentanoate (**13d**). Compound **12d** (0.29 g, 0.45 mmol) was reduced in the presence of NH_4Cl (0.057 g, 1.07 mmol) and zinc powder (0.041 g) as described for **13a**. Prep TLC with DCM:MeOH: NH_4OH (10:1:0.1) yielded **13c** (0.26 g, 92% yield). ^1H NMR (400 MHz, CDCl_3) δ 7.51–7.15 (m, 15H), 3.51–3.40 (m, 1H), 3.23–3.10 (m, 2H), 2.39–2.26 (m, 2H), 2.20–2.06 (m, 1H), 1.98–1.77 (m, 2H), 1.64–1.36 (m, 12H), 1.33–0.85 (m, 10H). ^{13}C NMR (101 MHz, CDCl_3) δ 177.4, 172.3, 141.9, 141.1, 129.0, 128.1, 127.9, 93.3, 82.0, 54.1, 39.5, 32.7, 31.2, 29.7, 29.4, 29.0, 28.8, 28.0, 26.7, 25.0, 23.3.

4.7.7.30. (*S*)-*Tert*-butyl 2-(4-(((2-amino-4-oxo-3,4-dihydropteridin-6-yl)methyl)amino)benzamido)-5-oxo-5-((4-oxo-4-((trityloxy)amino)butyl)amino)pentanoate (**14a**). Compound **13a** (0.078 g, 0.14 mmol) was coupled to pteroyl azide (0.13 g, 0.29 mmol) in presence of TMG (0.05 g, 0.43 mmol) in DMSO as described for **5** to yield **14a** (0.035 g, 29% yield). ¹H NMR (500 MHz, DMSO-*d*₆) δ 8.66 (s, 1H), 7.64 (d, *J* = 8.3 Hz, 2H), 7.32 (s, 16H), 6.64 (d, *J* = 8.4 Hz, 2H), 4.49 (d, *J* = 5.8 Hz, 2H), 4.24–4.15 (m, 1H), 2.85–2.75 (m, 2H), 2.17–2.11 (m, 2H), 2.04–1.95 (m, 1H), 1.92–1.82 (m, 1H), 1.79–1.72 (m, 2H), 1.40 (s, 9H), 1.34–1.27 (m, 2H). HRMS (ESI) calcd for C₄₆H₅₀N₉O₇ [M+H]⁺ 840.3828 found 840.3828.

4.7.7.31. (*S*)-*Tert*-butyl 2-(4-(((2-amino-4-oxo-3,4-dihydropteridin-6-yl)methyl)amino)benzamido)-5-oxo-5-((7-oxo-7-((trityloxy)amino)heptyl)amino)pentanoate (**14b**). Compound **13b** (0.22 g, 0.38 mmol) was coupled to pteroyl azide (0.16 g, 0.49 mmol) in presence of TMG (0.086 g, 0.75 mmol) in DMSO as described for **5** to yield **14b** (0.08 g, 24% yield). ¹H NMR (400 MHz, DMSO-*d*₆) δ 8.62 (s, 1H), 7.62 (d, *J* = 8.7 Hz, 2H), 7.30 (s, 19H), 6.61 (d, *J* = 8.9 Hz, 2H), 4.46 (d, *J* = 5.9 Hz, 2H), 4.24–4.13 (m, 1H), 2.97–2.88 (m, 2H), 2.18–2.10 (m, 2H), 2.02–1.93 (m, 1H), 1.92–1.82 (m, 1H), 1.74 (t, *J* = 7.7 Hz, 2H), 1.44–1.34 (m, 11H), 1.28–1.18 (m, 4H), 0.95–0.88 (m, 2H). HRMS (ESI) calcd for C₄₉H₅₆N₉O₇ [M+H]⁺ 882.4297 found 882.4295.

4.7.7.32. (*S*)-*Tert*-butyl 2-(4-(((2-amino-4-oxo-3,4-dihydropteridin-6-yl)methyl)amino)benzamido)-5-oxo-5-((8-oxo-8-((trityloxy)amino)octyl)amino)pentanoate (**14c**). Compound **13c** (0.20 g, 0.34 mmol) was coupled to pteroyl azide (0.23 g, 0.50 mmol) in presence of TMG (0.097 g, 0.84 mmol) in DMSO as described for **5** to yield **14c** (0.070 g, 23% yield). ¹H NMR (400 MHz, DMSO-*d*₆) δ 8.62 (s, 1H), 7.62 (d, *J* = 8.7 Hz, 2H), 7.30 (s, 15H), 6.61 (d, *J* = 8.7 Hz, 2H), 4.46 (d, *J* = 5.8 Hz, 2H), 4.22–4.14 (m, 1H), 3.01–2.91 (m, 2H), 2.15 (dd, *J* = 13.8, 6.8 Hz, 2H), 2.02–1.93 (m, 1H), 1.92–1.81 (m, 1H), 1.74 (t, *J* = 7.0 Hz, 2H), 1.36 (s, 9H), 1.32–1.24 (m, 2H), 1.17–1.04 (m, 6H), 0.94–0.81 (m, 2H). HRMS (ESI) calcd for C₅₀H₅₈N₉O₇ [M+H]⁺ 896.4454 found 896.4447.

4.7.7.33. (*S*)-*Tert*-butyl 2-(4-(((2-amino-4-oxo-3,4-dihydropteridin-6-yl)methyl)amino)benzamido)-5-oxo-5-((9-oxo-9-((trityloxy)amino)nonyl)amino)pentanoate (**14d**). Compound **13d** (0.25 g, 0.41 mmol) was coupled to pteroyl azide (0.21 g, 0.62 mmol) in presence of TMG (0.095 g, 0.82 mmol) in DMSO as described for **5** to yield **14d** (0.065 g, 17% yield). ¹H NMR (400 MHz, DMSO-*d*₆) δ 8.62 (s, 1H), 7.62 (d, *J* = 8.4 Hz, 2H), 7.30 (s, 12H), 6.61 (d, *J* = 8.5 Hz, 2H), 4.46 (d, *J* = 5.1 Hz, 2H), 4.26–4.11 (m, 1H), 3.00–2.94 (m, 2H), 2.21–2.09 (m, 2H), 2.06–1.93 (m, 1H), 1.91–1.79 (m, 1H), 1.74 (t, *J* = 8.6 Hz, 2H), 1.37 (s, 8H), 1.33–1.26 (m, 2H), 1.17–1.03 (m, 8H), 0.97–0.84 (m, 2H). HRMS (ESI) calcd for C₅₁H₆₀N₉O₇ [M+H]⁺ 910.4610 found 910.4603.

4.7.7.34. (*S*)-2-(4-(((2-Amino-4-oxo-3,4-dihydropteridin-6-yl)methyl)amino)benzamido)-5-((4-(hydroxyamino)-4-oxobutyl)amino)-5-oxopentanoic acid (**15a**). Compound **14a** (0.035 g, 0.042 mmol) was dissolved in neat TFA (2 mL) and TIPS (0.5 mL) and the resulting mixture was stirred at room temperature for 2 h. The desired product **15a** (0.022 g, 96% yield) was obtained as described for the synthesis of **6**. ¹H NMR (500 MHz, DMSO-*d*₆) δ 8.67 (s, 1H), 7.67 (d, *J* = 8.7 Hz, 2H), 6.65 (d, *J* = 8.7 Hz, 2H), 4.51 (s, 2H), 4.29 (t, *J* = 10.8 Hz, 1H), 3.01 (dt, *J* = 13.2, 6.8 Hz, 2H), 2.22–2.13 (m, 2H), 2.11–2.02 (m, 1H), 1.98–1.85 (m, 3H), 1.64–1.52 (m, 2H). ¹³C NMR (126 MHz, DMSO-*d*₆) δ 174.1, 171.7, 169.1, 166.6, 161.0, 153.8, 151.0, 149.4, 148.8, 129.3, 128.2, 121.6, 111.5, 52.4, 46.2, 38.4, 32.3, 30.2, 26.9, 25.6. HRMS (ESI) calcd for C₂₃H₂₈N₉O₇ [M+H]⁺ 542.2106 found 542.2097.

4.7.7.35. (*S*)-2-(4-(((2-Amino-4-oxo-3,4-dihydropteridin-6-yl)methyl)amino)benzamido)-5-((7-(hydroxyamino)-7-oxoheptyl)amino)-5-oxopentanoic acid (**15b**). Compound **14b** (0.061 g, 0.069 mmol) was dissolved in neat TFA (2 mL) and TIPS (0.5 mL) and the resulting mixture was stirred at room temperature for 2 h. The desired product **15b** (0.043 g, quantitative yield) was obtained as described for the synthesis of **6**. ¹H NMR (500 MHz, DMSO-*d*₆) δ 8.67 (s, 1H), 7.66 (d, *J* = 8.3 Hz, 2H), 6.65 (d, *J* = 8.2 Hz, 2H), 4.51 (s, 2H), 4.35–4.20 (m, 1H), 3.00 (dd, *J* = 12.1, 6.1 Hz, 2H), 2.22–2.14 (m, 2H), 2.11–2.01 (m, 1H), 1.97–1.85 (m, 3H), 1.52–1.41 (m, 2H), 1.39–1.30 (m, 2H), 1.28–1.16 (m, 4H). ¹³C NMR (126 MHz, DMSO-*d*₆) δ 174.1, 171.6, 166.6, 153.9, 151.0, 148.8, 129.3, 128.3, 121.7, 111.5, 52.5, 46.2, 38.8, 32.5, 32.3, 29.3, 28.6, 26.9, 26.4, 25.3. HRMS (ESI) calcd for C₂₆H₃₄N₉O₇ [M+H]⁺ 584.2576 found 584.2568.

4.7.7.36. (*S*)-2-(4-(((2-Amino-4-oxo-3,4-dihydropteridin-6-yl)methyl)amino)benzamido)-5-((8-(hydroxyamino)-8-oxooctyl)amino)-5-oxopentanoic acid (**15c**). Compound **14c** (0.07 g, 0.078 mmol) was dissolved in neat TFA (2 mL) and TIPS (0.5 mL) and the resulting mixture was stirred at room temperature for 2 h. The desired product **15c** (0.058 g, quantitative yield) was obtained as described for the synthesis of **6**. ¹H NMR (500 MHz, DMSO-*d*₆) δ 8.69 (s, 1H), 7.66 (d, *J* = 8.8 Hz, 2H), 6.65 (d, *J* = 8.8 Hz, 2H), 4.52 (s, 2H), 4.35–4.20 (m, 1H), 3.09–2.89 (m, 2H), 2.22–2.14 (m, 2H), 2.09–2.00 (m, 1H), 1.98–1.85 (m, 3H), 1.51–1.42 (m, 2H), 1.39–1.30 (m, 2H), 1.27–1.16 (m, 6H). ¹³C NMR (126 MHz, DMSO-*d*₆) δ 174.1, 171.6, 169.4, 166.5, 160.8, 153.6, 151.0, 149.8, 148.7, 129.2, 128.2, 121.7, 111.5, 52.6, 46.1, 38.8, 32.5, 32.3, 29.3, 28.8, 28.7, 26.9, 26.6, 25.4. HRMS (ESI) calcd for C₂₇H₃₆N₉O₇ [M+H]⁺ 598.2732 found 598.2717.

4.7.7.37. (*S*)-2-(4-(((2-Amino-4-oxo-3,4-dihydropteridin-6-yl)methyl)amino)benzamido)-5-((9-(hydroxyamino)-9-oxononyl)amino)-5-oxopentanoic acid (**15d**). Compound **14d** (0.065 g, 0.071 mmol) was dissolved in neat TFA (2 mL) and TIPS (2 mL) and the resulting mixture was stirred at room temperature for 2 h. The desired product **15d** (0.037 g, 84% yield) was obtained as described for the synthesis of **6**. ¹H NMR (500 MHz, DMSO-*d*₆) δ 8.67 (s, 1H), 7.66 (d, *J* = 8.7 Hz, 2H), 6.65 (d, *J* = 8.7 Hz, 2H), 4.51 (s, 2H), 4.34–4.20 (m, 1H), 3.00 (dd, *J* = 12.8, 6.7 Hz, 2H), 2.22–2.13 (m, 2H), 2.09–2.03 (m, 1H), 1.98–1.85 (m, 3H), 1.54–1.41 (m, 2H), 1.41–1.30 (m, 2H), 1.26–1.16 (m, 8H). ¹³C NMR (126 MHz, DMSO-*d*₆) δ 174.1, 171.6, 169.4, 166.5, 161.1, 155.6, 153.9, 151.0, 148.8, 129.2, 128.2, 121.6, 111.5, 52.6, 46.2, 38.8, 32.5, 32.3, 29.4, 29.0, 28.9, 28.8, 26.9, 26.7, 25.4. HRMS (ESI) calcd for C₂₈H₃₈N₉O₇ [M+H]⁺ 612.2889 found 612.2881.

4.7.7.38. *Tert*-butyl (2-(4-(thiophen-2-yl)phenyl)carbamate (**17**). Zinc powder (4.75 g) was added to a solution of **16** (6.65 g, 20.74 mmol) in dioxane (180 mL) and H₂O (45 mL) and stirred overnight at 70 °C. Upon completion, EtOAc was added and the mixture was washed with H₂O (3 × 100 mL) and brine (1 × 100 mL). The crude product was purified by column chromatography, eluting with EtOAc:Hexanes (2:1), to obtain **17** (3.95 g, 54% yield). ¹H NMR (400 MHz, CDCl₃) δ 7.34–7.20 (m, 3H), 7.10–6.98 (m, 3H), 1.52 (s, 9H). ¹³C NMR (101 MHz, CDCl₃) δ 153.7, 144.1, 139.9, 132.2, 127.9, 124.8, 124.4, 122.8, 117.5, 115.0, 80.7, 28.3.

4.7.7.39. *Tert*-butyl (2-(4-(azidobutanamido)-4-(thiophen-2-yl)phenyl)carbamate (**19a**). The azido carboxylic acid **18a** (0.31 g, 2.41 mmol), EDCI (0.46 g, 2.41 mmol) and HOBt (0.33 g, 2.41 mmol) were dissolved in DMF and the mixture was stirred at room temperature for 30 min. Following the addition of **17** (0.5 g, 1.72 mmol), the reaction was allowed to stir at 70 °C for 6 h. Once the reaction was completed, DCM was added and the mixture was washed with

H₂O (3 × 50 mL), NaHCO₃ (1 × 50 mL), brine (1 × 50 mL) and dried with Na₂SO₄. Solvent was evaporated off to give **19a** (0.64 g, 92% yield) which was used without further purification. ¹H NMR (400 MHz, CDCl₃) δ 7.42–7.31 (m, 2H), 7.28–7.19 (m, 2H), 7.04 (dd, *J* = 5.1, 3.6 Hz, 1H), 6.98 (s, 1H), 3.34 (t, *J* = 6.6 Hz, 2H), 2.42 (t, *J* = 7.2 Hz, 2H), 1.95 (p, *J* = 6.9 Hz, 2H), 1.51 (s, 9H). ¹³C NMR (101 MHz, CDCl₃) δ 171.3, 154.1, 143.1, 131.5, 130.1, 129.8, 128.1, 124.9, 124.6, 123.7, 123.3, 122.6, 81.1, 50.7, 33.7, 28.3, 24.7.

4.7.7.40. Tert-butyl (2-(7-azidoheptanamido)-4-(thiophen-2-yl)phenyl)carbamate (19b). The azido carboxylic acid **18b** (0.41 g, 2.4 mmol) was coupled to **17** (0.5 g, 1.72 mmol) in the presence of EDCI (0.46 g, 2.41 mmol) and HOBT (0.33 g, 2.41 mmol) as described for **19a** to give **19b** (0.74 g, 98% yield) which was used without further purification. ¹H NMR (400 MHz, CDCl₃) δ 7.40 (d, *J* = 8.4 Hz, 1H), 7.33 (dd, *J* = 8.4, 1.9 Hz, 1H), 7.21 (ddd, *J* = 12.5, 8.3, 4.9 Hz, 3H), 7.07–6.95 (m, 1H), 3.22 (t, *J* = 6.9 Hz, 2H), 2.31 (t, *J* = 7.5 Hz, 2H), 1.74–1.61 (m, 2H), 1.60–1.51 (m, 2H), 1.49 (s, 9H), 1.34 (t, *J* = 9.5 Hz, 4H). ¹³C NMR (101 MHz, CDCl₃) δ 172.6, 154.1, 143.2, 131.3, 130.3, 129.9, 128.0, 124.7, 124.6, 123.5, 123.2, 122.5, 80.8, 51.3, 36.9, 28.7, 28.3, 26.4, 25.4.

4.7.7.41. Tert-butyl (2-(8-azidooctanamido)-4-(thiophen-2-yl)phenyl)carbamate (19c). The azido carboxylic acid **18c** (0.45 g, 2.4 mmol) was coupled to **17** (0.5 g, 1.72 mmol) in the presence of EDCI (0.46 g, 2.41 mmol) and HOBT (0.33 g, 2.41 mmol) as described for **19a** to give **19c** (0.56 g, 72% yield) which was used without further purification. ¹H NMR (500 MHz, CDCl₃) δ 7.45–7.34 (m, 2H), 7.30–7.23 (m, 2H), 7.06 (dd, *J* = 8.9, 5.0 Hz, 2H), 3.27 (t, *J* = 6.9 Hz, 2H), 2.36 (t, *J* = 7.5 Hz, 2H), 1.76–1.66 (m, 2H), 1.65–1.56 (m, 2H), 1.53 (s, 9H), 1.42–1.31 (m, 6H). ¹³C NMR (126 MHz, CDCl₃) δ 172.4, 154.0, 143.1, 131.4, 129.9, 127.9, 124.6, 124.5, 123.4, 123.1, 122.4, 80.8, 51.3, 36.9, 28.9, 28.7, 28.6, 28.1, 26.4, 25.3.

4.7.7.42. Tert-butyl (2-(9-azidononanamido)-4-(thiophen-2-yl)phenyl)carbamate (19d). The azido carboxylic acid **18d** (0.48 g, 2.41 mmol) was coupled to **17** (0.5 g, 1.72 mmol) in the presence of EDCI (0.46 g, 2.41 mmol) and HOBT (0.33 g, 2.41 mmol) as described for **19a**. The crude product was purified by column chromatography using DCM:Acetone (30:1) as eluent to obtain **19d** (0.56 g, 70% yield). ¹H NMR (400 MHz, CDCl₃) δ 7.29 (dt, *J* = 8.4, 5.1 Hz, 2H), 7.16 (ddd, *J* = 5.5, 4.4, 1.1 Hz, 2H), 7.02–6.91 (m, 2H), 3.18 (t, *J* = 6.9 Hz, 2H), 2.27 (t, *J* = 7.5 Hz, 2H), 1.67–1.57 (m, 2H), 1.55–1.48 (m, 2H), 1.43 (s, 8H), 1.33–1.18 (m, 8H). ¹³C NMR (101 MHz, CDCl₃) δ 172.6, 154.1, 143.2, 131.5, 130.1, 128.0, 124.8, 124.7, 123.6, 123.2, 122.6, 80.9, 51.4, 37.1, 29.2, 29.1, 29.0, 28.8, 28.3, 26.7, 25.6.

4.7.7.43. Tert-butyl (2-(4-aminobutanamido)-4-(thiophen-2-yl)phenyl)carbamate (20a). To a solution of **19a** (0.53 g, 1.37 mmol) in EtOH (9 mL), EtOAc (3 mL) and H₂O (3 mL), NH₄Cl (0.18 g, 3.42 mmol) and zinc powder (0.23 g) were added and the resulting mixture was stirred under reflux for 2 h. After completion of the reaction, the mixture was filtered through a celite pad. The crude product was purified by preparative TLC with DCM:MeOH:NH₄OH (8.5:1.5:0.3) yielding **20a** (0.40 g, 78% yield). ¹H NMR (400 MHz, CDCl₃) δ 7.66–7.45 (m, 2H), 7.31 (d, *J* = 8.1 Hz, 1H), 7.15 (s, 2H), 6.97 (s, 1H), 2.80–2.53 (m, 2H), 2.42–2.29 (m, 2H), 1.86–1.69 (m, 2H), 1.52–1.38 (m, 9H). ¹³C NMR (101 MHz, CDCl₃) δ 172.8, 153.9, 143.3, 131.2, 130.6, 129.1, 128.0, 124.6, 124.0, 123.7, 123.0, 122.6, 80.6, 40.8, 34.4, 28.3, 27.3.

4.7.7.44. Tert-butyl (2-(7-aminoheptanamido)-4-(thiophen-2-yl)phenyl)carbamate (20b). Compound **19b** (0.55 g, 1.24 mmol) was reduced with NH₄Cl (0.16 g, 2.98 mmol) and zinc (0.21 g) as described for **20a** resulting in **20b** (0.38 g, 74% yield). ¹H NMR

(400 MHz, CDCl₃) δ 7.58 (s, 1H), 7.41 (d, *J* = 8.4 Hz, 1H), 7.30 (d, *J* = 8.4 Hz, 1H), 7.17 (t, *J* = 3.8 Hz, 2H), 7.02–6.89 (m, 1H), 2.70–2.48 (m, 2H), 2.27 (t, *J* = 7.2 Hz, 2H), 1.67–1.53 (m, 2H), 1.45 (s, 9H), 1.36 (d, *J* = 5.6 Hz, 2H), 1.29–1.15 (m, 4H). ¹³C NMR (101 MHz, CDCl₃) δ 172.9, 154.1, 143.3, 131.1, 130.5, 130.0, 128.0, 124.7, 124.5, 123.4, 123.1, 122.5, 80.6, 41.7, 36.8, 32.7, 28.8, 28.3, 26.4, 25.5.

4.7.7.45. Tert-butyl (2-(8-aminooctanamido)-4-(thiophen-2-yl)phenyl)carbamate (20c). Compound **19c** (0.40 g, 0.87 mmol) was reduced with NH₄Cl (0.12 g, 2.19 mmol) and zinc (0.14 g) as described for **20a** resulting in **20c** (0.32 g, 86% yield). ¹H NMR (400 MHz, CDCl₃) δ 7.55 (s, 1H), 7.38 (d, *J* = 7.6 Hz, 1H), 7.26 (d, *J* = 3.4 Hz, 1H), 7.19–7.04 (m, 2H), 6.94 (s, 1H), 2.64–2.47 (m, 2H), 2.32–2.15 (m, 2H), 1.67–1.49 (m, 2H), 1.42 (s, 9H), 1.27–0.93 (m, 8H). ¹³C NMR (101 MHz, CDCl₃) δ 173.0, 154.1, 143.2, 131.1, 130.5, 130.0, 128.0, 124.6, 123.4, 123.0, 122.4, 80.5, 41.7, 36.9, 32.7, 28.9, 28.3, 26.5, 25.5.

4.7.7.46. Tert-butyl (2-(9-aminononanamido)-4-(thiophen-2-yl)phenyl)carbamate (20d). Compound **19d** (0.45 g, 0.95 mmol) was reduced with NH₄Cl (0.13 g, 2.39 mmol) and zinc (0.16 g) as described for **20a** resulting in **20d** (0.34 g, 79% yield). ¹H NMR (400 MHz, CDCl₃) δ 7.60 (s, 1H), 7.38 (d, *J* = 8.4 Hz, 1H), 7.30 (d, *J* = 8.2 Hz, 1H), 7.19 (d, *J* = 5.7 Hz, 2H), 7.04–6.91 (m, 1H), 2.63 (t, *J* = 8.7 Hz, 2H), 2.30 (t, *J* = 7.2 Hz, 2H), 1.73–1.56 (m, 2H), 1.46 (s, 9H), 1.41 (s, 2H), 1.24 (s, 8H). ¹³C NMR (101 MHz, CDCl₃) δ 172.9, 154.2, 143.3, 131.2, 130.4, 130.1, 128.0, 124.7, 124.6, 123.4, 123.1, 122.5, 80.6, 41.7, 37.0, 32.5, 29.1, 29.1, 29.0, 28.3, 26.7, 25.6.

4.7.7.47. (S)-Tert-butyl 2-azido-5-((4-((2-((tert-butoxycarbonyl)amino)-5-(thiophen-2-yl)phenyl)amino)-4-oxobutyl)amino)-5-oxopentanoate (21a). The α-azido L-glutamic acid α-tert-butyl ester **1** (0.13 g, 0.56 mmol), EDCI (0.11 g, 0.56 mmol) and HOBT (0.076 g, 0.56 mmol) were dissolved in DMF and stirred at room temperature for 30 min. Compound **20a** (0.15 g, 0.34 mmol) was added and the mixture allowed to stir overnight at room temperature. DCM was added to the reaction and then washed with H₂O (3 × 50 mL), NaHCO₃ (1 × 50 mL), brine (1 × 50 mL) and dried with Na₂SO₄. Solvent was evaporated off and the crude product was purified by preparative TLC using DCM:MeOH:NH₄OH (8.5:1.5:0.3) to yield **21a** (0.23 g, 98% yield). ¹H NMR (400 MHz, CDCl₃) δ 7.59–7.49 (m, 2H), 7.36 (dd, *J* = 8.4, 1.7 Hz, 1H), 7.20 (t, *J* = 3.7 Hz, 2H), 7.00 (dd, *J* = 4.8, 3.8 Hz, 1H), 3.78 (dd, *J* = 8.7, 4.8 Hz, 1H), 3.29–3.20 (m, 2H), 2.36 (t, *J* = 11.1 Hz, 2H), 2.25 (t, *J* = 7.1 Hz, 2H), 2.18–2.04 (m, 1H), 2.00–1.89 (m, 1H), 1.86–1.75 (m, 2H), 1.47 (s, 9H), 1.45 (s, 9H). ¹³C NMR (101 MHz, CDCl₃) δ 172.4, 169.2, 153.9, 143.2, 131.0, 130.5, 129.5, 128.0, 124.7, 124.4, 123.6, 123.1, 122.3, 83.1, 80.7, 61.8, 38.7, 34.2, 32.1, 28.3, 28.0, 27.0, 25.9.

4.7.7.48. (S)-Tert-butyl 2-azido-5-((7-((2-((tert-butoxycarbonyl)amino)-5-(thiophen-2-yl)phenyl)amino)-7-oxoheptyl)amino)-5-oxopentanoate (21b). Compound **1** (0.12 g, 0.50 mmol) was coupled to **20b** (0.15 g, 0.36 mmol) with EDCI (0.096 g, 0.50 mmol) and HOBT (0.068 g, 0.50 mmol) as described for **21a** to give **21b** (0.22 g, 98% yield). ¹H NMR (400 MHz, CDCl₃) δ 7.57–7.44 (m, 2H), 7.33 (d, *J* = 8.4 Hz, 1H), 7.18 (d, *J* = 4.5 Hz, 2H), 7.03–6.90 (m, 1H), 3.76 (dd, *J* = 8.9, 4.8 Hz, 1H), 3.10 (dd, *J* = 12.9, 6.6 Hz, 2H), 2.30 (t, *J* = 7.2 Hz, 2H), 2.22 (t, *J* = 7.2 Hz, 2H), 2.17–2.05 (m, 1H), 1.96–1.83 (m, 1H), 1.64–1.54 (m, 2H), 1.45 (s, 9H), 1.44 (s, 9H), 1.41–1.32 (m, 2H), 1.30–1.18 (m, 4H). ¹³C NMR (101 MHz, CDCl₃) δ 172.9, 171.6, 169.2, 154.0, 143.2, 131.1, 130.5, 129.8, 128.0, 124.7, 124.5, 123.4, 123.1, 122.5, 83.0, 80.7, 61.8, 39.3, 36.7, 32.1, 29.2, 28.5, 28.3, 27.9, 27.1, 26.3, 25.4.

4.7.7.49. (*S*)-*Tert*-butyl 2-azido-5-((8-((2-((*tert*-butoxycarbonyl)amino)-5-(thiophen-2-yl)phenyl)amino)-8-oxooctyl)amino)-5-oxopentanoate (**21c**). Compound **1** (0.11 g, 0.49 mmol) was coupled to **20c** (0.15 g, 0.35 mmol) with EDCI (0.093 g, 0.49 mmol) and HOBT (0.066 g, 0.49 mmol) as described for **21a** to give **21c** (0.23 g, quantitative yield). ¹H NMR (400 MHz, CDCl₃) δ 7.53–7.41 (m, 2H), 7.39–7.30 (m, 1H), 7.18 (t, *J* = 3.8 Hz, 2H), 6.99 (dd, *J* = 4.9, 3.8 Hz, 1H), 3.76 (dd, *J* = 9.0, 4.8 Hz, 1H), 3.13 (dd, *J* = 13.4, 6.7 Hz, 2H), 2.32 (t, *J* = 7.3 Hz, 2H), 2.21 (t, *J* = 7.2 Hz, 2H), 2.15–2.03 (m, 1H), 1.89 (ddd, *J* = 15.6, 13.9, 6.9 Hz, 1H), 1.71–1.57 (m, 2H), 1.46 (s, 9H), 1.44 (s, 9H), 1.42–1.37 (m, 2H), 1.31–1.22 (m, 6H). ¹³C NMR (101 MHz, CDCl₃) δ 172.8, 171.5, 169.2, 154.0, 143.3, 131.1, 130.4, 129.9, 128.0, 124.7, 124.5, 123.4, 123.1, 122.5, 83.0, 80.7, 61.8, 39.4, 36.9, 32.1, 29.3, 28.8, 28.6, 28.3, 28.0, 27.1, 26.5, 25.4.

4.7.7.50. (*S*)-*Tert*-butyl 2-azido-5-((9-((2-((*tert*-butoxycarbonyl)amino)-5-(thiophen-2-yl)phenyl)amino)-9-oxononyl)amino)-5-oxopentanoate (**21d**). Compound **1** (0.087 g, 0.38 mmol) was coupled to **20d** (0.15 g, 0.27 mmol) with EDCI (0.072 g, 0.38 mmol) and HOBT (0.051 g, 0.38 mmol) as described for **21a** to give **21d** (0.20 g, quantitative yield). ¹H NMR (400 MHz, CDCl₃) δ 7.43 (dd, *J* = 15.0, 9.4 Hz, 2H), 7.34 (dd, *J* = 8.4, 2.0 Hz, 1H), 7.20 (dd, *J* = 4.1, 2.9 Hz, 2H), 7.00 (dd, *J* = 4.9, 3.7 Hz, 1H), 3.77 (dd, *J* = 9.0, 4.8 Hz, 1H), 3.16 (dd, *J* = 13.6, 6.5 Hz, 2H), 2.34 (t, *J* = 7.4 Hz, 2H), 2.22 (t, *J* = 7.1 Hz, 2H), 2.17–2.07 (m, 1H), 1.97–1.85 (m, 1H), 1.71–1.61 (m, 2H), 1.47 (s, 9H), 1.45 (s, 9H), 1.43–1.39 (m, 2H), 1.30–1.18 (m, 8H). ¹³C NMR (101 MHz, CDCl₃) δ 172.8, 171.4, 169.2, 154.0, 143.3, 131.2, 130.4, 130.0, 128.0, 124.7, 124.5, 123.5, 123.1, 122.5, 83.1, 80.7, 61.8, 39.5, 37.0, 32.1, 29.4, 28.9, 28.8, 28.3, 28.0, 27.1, 26.6, 25.5.

4.7.7.51. (*S*)-*Tert*-butyl 2-amino-5-((4-((2-((*tert*-butoxycarbonyl)amino)-5-(thiophen-2-yl)phenyl)amino)-4-oxobutyl)amino)-5-oxopentanoate (**22a**). To a solution of **21a** (0.21 g, 0.37 mmol) in EtOH (9 mL) and H₂O (3 mL) was added NH₄Cl (0.049 g, 0.91 mmol) and zinc powder (0.06 g) and the resulting mixture was stirred under reflux for 3 h. After completion of the reaction, the mixture was filtered through a celite pad. The crude product was purified by preparative TLC with DCM:MeOH (10:1) yielding **22a** (0.13 g, 63% yield). ¹H NMR (400 MHz, CDCl₃) δ 7.72 (s, 1H), 7.55 (d, *J* = 8.3 Hz, 1H), 7.38 (d, *J* = 8.4 Hz, 1H), 7.23 (dd, *J* = 8.9, 8.1 Hz, 2H), 7.06–6.98 (m, 1H), 3.36–3.20 (m, 3H), 2.39 (t, *J* = 6.2 Hz, 2H), 2.32–2.24 (m, 2H), 2.14–2.06 (m, 1H), 1.93–1.83 (m, 2H), 1.79–1.70 (m, 1H), 1.49 (s, 9H), 1.43 (s, 9H). ¹³C NMR (101 MHz, CDCl₃) δ 172.3, 154.0, 143.4, 131.1, 130.4, 129.8, 128.0, 124.7, 123.6, 123.1, 122.4, 81.5, 80.6, 38.6, 34.3, 33.0, 28.3, 28.0, 26.1.

4.7.7.52. (*S*)-*Tert*-butyl 2-amino-5-((7-((2-((*tert*-butoxycarbonyl)amino)-5-(thiophen-2-yl)phenyl)amino)-7-oxoheptyl)amino)-5-oxopentanoate (**22b**). Compound **21b** (0.22 g, 0.34 mmol) was reduced in the presence of NH₄Cl (0.046 g, 0.86 mmol) and zinc powder (0.056 g) as described for **22a** yielding **22b** (0.14 g, 68% yield). ¹H NMR (400 MHz, CDCl₃) δ 7.42 (dd, *J* = 31.0, 8.4 Hz, 3H), 7.29–7.18 (m, 2H), 7.10–6.94 (m, 1H), 3.29–3.07 (m, 2H), 2.37 (t, *J* = 5.5 Hz, 2H), 2.32–2.19 (m, 2H), 2.15–1.99 (m, 1H), 1.85–1.63 (m, 4H), 1.61–1.39 (m, 20H), 1.39–1.27 (m, 4H). ¹³C NMR (101 MHz, CDCl₃) δ 172.5, 143.3, 131.5, 130.2, 128.0, 124.8, 123.6, 123.2, 122.6, 81.4, 80.8, 39.2, 36.8, 33.1, 29.3, 28.3, 28.0, 26.2, 25.3.

4.7.7.53. (*S*)-*Tert*-butyl 2-amino-5-((8-((2-((*tert*-butoxycarbonyl)amino)-5-(thiophen-2-yl)phenyl)amino)-8-oxooctyl)amino)-5-oxopentanoate (**22c**). Compound **21c** (0.23 g, 0.36 mmol) was reduced in the presence of NH₄Cl (0.086 g, 1.61 mmol) and zinc powder (0.11 g) as described for **22a** yielding **22c** (0.20 g, 90% yield). ¹H NMR (400 MHz, CDCl₃) δ 7.59 (s, 1H), 7.45 (d, *J* = 8.4 Hz, 1H), 7.34 (d, *J* = 8.3 Hz, 1H), 7.20 (d, *J* = 4.3 Hz, 2H), 7.06–6.93 (m, 1H),

3.20–3.07 (m, 2H), 2.99–2.75 (m, 2H), 2.35 (t, *J* = 7.1 Hz, 2H), 2.25 (t, *J* = 14.4 Hz, 2H), 2.04 (dd, *J* = 20.4, 9.4 Hz, 1H), 1.84–1.72 (m, 1H), 1.70–1.61 (m, 2H), 1.47 (s, 9H), 1.40 (s, 9H), 1.34–1.18 (m, 6H). ¹³C NMR (101 MHz, CDCl₃) δ 172.9, 154.1, 143.3, 131.2, 130.4, 130.1, 128.0, 125.0, 123.5, 123.1, 122.6, 82.0, 80.7, 77.4, 77.1, 76.8, 50.4, 39.4, 36.9, 32.7, 29.2, 28.7, 28.4, 28.3, 28.0, 26.4, 25.4.

4.7.7.54. (*S*)-*Tert*-butyl 2-amino-5-((9-((2-((*tert*-butoxycarbonyl)amino)-5-(thiophen-2-yl)phenyl)amino)-9-oxononyl)amino)-5-oxopentanoate (**22d**). Compound **21d** (0.20 g, 0.30 mmol) was reduced in the presence of NH₄Cl (0.073 g, 1.36 mmol) and zinc powder (0.089 g) as described for **22a** yielding **22d** (0.17 g, 88% yield). ¹H NMR (400 MHz, CDCl₃) δ 7.58 (s, 1H), 7.44 (t, *J* = 11.0 Hz, 1H), 7.32 (dd, *J* = 8.4, 1.6 Hz, 1H), 7.22–7.13 (m, 2H), 7.04–6.92 (m, 1H), 3.18–3.03 (m, 2H), 2.34 (t, *J* = 7.3 Hz, 2H), 2.31–2.20 (m, 2H), 2.10–1.94 (m, 1H), 1.87–1.70 (m, 1H), 1.71–1.60 (m, 2H), 1.46 (s, 9H), 1.41 (m, 10H), 1.36–1.15 (m, 9H). ¹³C NMR (101 MHz, CDCl₃) δ 173.0, 154.1, 143.3, 131.1, 130.5, 130.0, 128.0, 124.7, 124.5, 123.4, 123.1, 122.5, 81.9, 80.6, 39.4, 36.9, 32.7, 29.3, 28.8, 28.7, 28.3, 28.0, 26.5, 25.5.

4.7.7.55. (*S*)-*Tert*-butyl 2-(4-(((2-amino-4-oxo-3,4-dihydropteridin-6-yl)methyl)amino)benzamido)-5-(((2-((*tert*-butoxycarbonyl)amino)-5-(thiophen-2-yl)phenyl)amino)-4-oxobutyl)amino)-5-oxopentanoate (**23a**). Compound **22a** (0.12 g, 0.21 mmol) was coupled to pteroyl azide (0.19 g, 0.41 mmol) in the presence of TMG (0.071 g, 0.62 mmol) in DMSO as described for the synthesis of **5** to yield **23a** (0.045 g, 26% yield). ¹H NMR (500 MHz, DMSO-*d*₆) δ 8.66 (s, 1H), 7.75 (d, *J* = 1.9 Hz, 1H), 7.67 (d, *J* = 8.8 Hz, 2H), 7.62 (d, *J* = 8.5 Hz, 1H), 7.52 (dd, *J* = 5.1, 1.0 Hz, 1H), 7.48–7.38 (m, 2H), 7.12 (dd, *J* = 5.0, 3.6 Hz, 1H), 6.66 (dd, *J* = 14.6, 8.9 Hz, 2H), 4.49 (d, *J* = 6.0 Hz, 2H), 4.24 (dd, *J* = 12.3, 9.4 Hz, 1H), 3.15–3.08 (m, 2H), 2.38 (t, *J* = 7.3 Hz, 2H), 2.21 (dt, *J* = 14.2, 7.1 Hz, 2H), 2.09–1.99 (m, 1H), 1.97–1.87 (m, 1H), 1.74 (dd, *J* = 16.3, 9.0 Hz, 2H), 1.46 (s, 9H), 1.40 (s, 9H). HRMS (ESI) calcd for C₄₂H₅₁N₁₀O₈S [M+H]⁺ 855.3607 found 855.3607.

4.7.7.56. (*S*)-*Tert*-butyl 2-(4-(((2-amino-4-oxo-3,4-dihydropteridin-6-yl)methyl)amino)benzamido)-5-(((7-((2-((*tert*-butoxycarbonyl)amino)-5-(thiophen-2-yl)phenyl)amino)-7-oxoheptyl)amino)-5-oxopentanoate (**23b**). Compound **22b** (0.12 g, 0.20 mmol) was coupled to pteroyl azide (0.18 g, 0.41 mmol) in the presence of TMG (0.07 g, 0.61 mmol) in DMSO as described for the synthesis of **5** to yield **23b** (0.038 g, 21% yield). ¹H NMR (500 MHz, DMSO-*d*₆) δ 8.66 (s, 1H), 7.73 (d, *J* = 1.9 Hz, 1H), 7.66 (d, *J* = 8.8 Hz, 2H), 7.61 (d, *J* = 8.4 Hz, 1H), 7.52 (dd, *J* = 5.1, 1.1 Hz, 1H), 7.47–7.40 (m, 2H), 7.13 (dd, *J* = 4.5, 3.0 Hz, 1H), 6.65 (d, *J* = 8.8 Hz, 2H), 4.49 (d, *J* = 5.9 Hz, 2H), 4.24–4.16 (m, 1H), 3.03 (dd, *J* = 12.9, 6.7 Hz, 2H), 2.40–2.35 (m, 2H), 2.24–2.12 (m, 2H), 2.06–1.97 (m, 1H), 1.94–1.85 (m, 1H), 1.65–1.54 (m, 2H), 1.47 (s, 10H), 1.42–1.36 (m, 12H), 1.35–1.27 (m, 4H). HRMS (ESI) calcd for C₄₅H₅₇N₁₀O₈S [M+H]⁺ 897.4076 found 897.4072.

4.7.7.57. (*S*)-*Tert*-butyl 2-(4-(((2-amino-4-oxo-3,4-dihydropteridin-6-yl)methyl)amino)benzamido)-5-(((8-((2-((*tert*-butoxycarbonyl)amino)-5-(thiophen-2-yl)phenyl)amino)-8-oxooctyl)amino)-5-oxopentanoate (**23c**). Compound **22c** (0.17 g, 0.28 mmol) was coupled to pteroyl azide (0.25 g, 0.56 mmol) in the presence of TMG (0.097 g, 0.84 mmol) in DMSO as described for the synthesis of **5** to yield **23c** (0.070 g, 28% yield). ¹H NMR (400 MHz, DMSO-*d*₆) δ 8.58 (s, 1H), 7.71 (s, 1H), 7.62 (d, *J* = 8.6 Hz, 2H), 7.58 (d, *J* = 8.7 Hz, 1H), 7.49 (d, *J* = 4.5 Hz, 1H), 7.44–7.37 (m, 2H), 7.12–7.08 (m, 1H), 6.61 (d, *J* = 8.5 Hz, 2H), 4.44 (d, *J* = 6.0 Hz, 2H), 4.23–4.12 (m, 1H), 3.03–2.94 (m, 2H), 2.34 (t, *J* = 7.5 Hz, 2H), 2.20–2.11 (m, 2H), 2.02–1.94 (m, 1H), 1.91–1.82 (m, 1H), 1.62–1.54 (m, 2H), 1.42 (s, 9H), 1.37 (s, 9H), 1.32–1.20 (m, 8H). HRMS (ESI) calcd for C₄₆H₅₉N₁₀O₈S [M+H]⁺

911.4233 found 911.4217.

4.7.7.58. (*S*)-*Tert*-butyl 2-(4-(((2-amino-4-oxo-3,4-dihydropteridin-6-yl)methyl)amino)benzamido)-5-((9-((2-((*tert*-butoxycarbonyl)amino)-5-(thiophen-2-yl)phenyl)amino)-9-oxononyl)amino)-5-oxopentanoate (**23d**). Compound **22d** (0.17 g, 0.27 mmol) was coupled to pteroyl azide (0.24 g, 0.53 mmol) in the presence of TMG (0.091 g, 0.80 mmol) in DMSO as described for the synthesis of **5** to yield **23d** (0.11 g, 46% yield). ¹H NMR (400 MHz, DMSO-*d*₆) δ 8.63 (s, 1H), 7.69 (d, *J* = 2.1 Hz, 1H), 7.63 (d, *J* = 8.8 Hz, 2H), 7.57 (d, *J* = 8.5 Hz, 1H), 7.49 (d, *J* = 5.1 Hz, 1H), 7.45–7.36 (m, 2H), 7.10 (dd, *J* = 5.0, 3.7 Hz, 1H), 6.62 (d, *J* = 8.8 Hz, 2H), 4.46 (d, *J* = 6.0 Hz, 2H), 4.23–4.12 (m, 1H), 3.02–2.94 (m, 2H), 2.34 (t, *J* = 7.5 Hz, 2H), 2.15 (dd, *J* = 12.6, 6.6 Hz, 2H), 2.01–1.93 (m, 1H), 1.91–1.83 (m, 1H), 1.64–1.54 (m, 2H), 1.44 (s, 9H), 1.41–1.38 (m, 2H), 1.37 (s, 9H), 1.32–1.21 (m, 8H). HRMS (ESI) calcd for C₄₇H₆₁N₁₀O₆S [M+H]⁺ 925.4389 found 925.4386.

4.7.7.59. (*S*)-2-(4-(((2-Amino-4-oxo-3,4-dihydropteridin-6-yl)methyl)amino)benzamido)-5-((4-((2-amino-5-(thiophen-2-yl)phenyl)amino)-4-oxobutyl)amino)-5-oxopentanoic acid (**24a**). Compound **23a** (0.032 g, 0.037 mmol) was dissolved in neat TFA (2 mL) and TIPS (0.5 mL) and stirred at room temperature for 2 h. The desired product **24a** (0.03 g, quantitative yield) was obtained as described for the synthesis of **6**. ¹H NMR (500 MHz, DMSO-*d*₆) δ 8.66 (s, 1H), 7.67 (d, *J* = 8.5 Hz, 2H), 7.50 (s, 1H), 7.36 (d, *J* = 4.8 Hz, 1H), 7.27–7.18 (m, 2H), 7.07–7.03 (m, 1H), 6.77 (d, *J* = 8.3 Hz, 1H), 6.65 (d, *J* = 8.5 Hz, 2H), 4.50 (s, 2H), 4.32 (t, *J* = 10.6 Hz, 1H), 3.11 (dt, *J* = 12.8, 6.7 Hz, 2H), 2.33 (t, *J* = 7.4 Hz, 2H), 2.22 (t, *J* = 7.3 Hz, 2H), 2.14–2.06 (m, 1H), 1.99–1.88 (m, 1H), 1.78–1.65 (m, 2H). ¹³C NMR (126 MHz, DMSO-*d*₆) δ 174.1, 171.8, 171.4, 166.7, 153.9, 151.0, 148.8, 144.5, 129.3, 128.5, 124.1, 123.6, 123.5, 122.9, 121.6, 121.3, 116.6, 111.5, 65.2, 52.4, 46.2, 38.3, 33.4, 32.3, 31.0, 26.9, 25.6, 15.5. HRMS (ESI) calcd for C₃₃H₃₅N₁₀O₆S [M+H]⁺ 699.2456 found 699.2450.

4.7.7.60. (*S*)-2-(4-(((2-Amino-4-oxo-3,4-dihydropteridin-6-yl)methyl)amino)benzamido)-5-((7-((2-amino-5-(thiophen-2-yl)phenyl)amino)-7-oxoheptyl)amino)-5-oxopentanoic acid (**24b**). Compound **23b** (0.039 g, 0.043 mmol) was dissolved in neat TFA (2 mL) and TIPS (0.5 mL) and stirred at room temperature for 2 h. The desired product **24b** (0.027 g, 84% yield) was obtained as described for the synthesis of **6**. ¹H NMR (500 MHz, DMSO-*d*₆) δ 8.67 (s, 1H), 7.67 (d, *J* = 8.6 Hz, 2H), 7.51 (d, *J* = 1.8 Hz, 1H), 7.36 (d, *J* = 4.9 Hz, 1H), 7.26–7.20 (m, 2H), 7.07–7.03 (m, 1H), 6.79 (d, *J* = 8.2 Hz, 1H), 6.65 (d, *J* = 8.6 Hz, 2H), 4.50 (s, 2H), 4.28 (t, *J* = 10.9 Hz, 1H), 3.08–2.99 (m, 2H), 2.34 (t, *J* = 7.4 Hz, 2H), 2.19 (t, *J* = 8.4 Hz, 2H), 2.08–2.02 (m, 1H), 1.97–1.88 (m, 1H), 1.65–1.53 (m, 2H), 1.43–1.34 (m, 2H), 1.35–1.25 (m, 4H). ¹³C NMR (126 MHz, DMSO-*d*₆) δ 174.1, 171.6, 166.6, 151.0, 148.8, 144.5, 129.3, 128.5, 128.2, 123.6, 122.7, 121.6, 121.4, 111.5, 65.2, 52.6, 46.2, 38.8, 36.1, 32.3, 29.3, 28.7, 26.9, 26.5, 25.4, 15.5. HRMS (ESI) calcd for C₃₆H₄₁N₁₀O₆S [M+H]⁺ 741.2926 found 741.2922.

4.7.7.61. (*S*)-2-(4-(((2-Amino-4-oxo-3,4-dihydropteridin-6-yl)methyl)amino)benzamido)-5-((8-((2-amino-5-(thiophen-2-yl)phenyl)amino)-8-oxooctyl)amino)-5-oxopentanoic acid (**24c**). Compound **23c** (0.032 g, 0.035 mmol) was dissolved in neat TFA (2 mL) and TIPS (0.5 mL) and stirred at room temperature for 2 h. The desired product **24c** (0.025 g, 93% yield) was obtained as described for the synthesis of **6**. ¹H NMR (500 MHz, DMSO-*d*₆) δ 8.67 (s, 1H), 7.66 (d, *J* = 8.8 Hz, 2H), 7.51 (d, *J* = 1.9 Hz, 1H), 7.37 (d, *J* = 4.6 Hz, 1H), 7.27–7.21 (m, 2H), 7.07–7.03 (m, 2H), 6.79 (t, *J* = 7.3 Hz, 1H), 6.65 (d, *J* = 8.8 Hz, 2H), 4.51 (s, 2H), 4.32–4.23 (m, 1H), 3.08–2.99 (m, 2H), 2.34 (dd, *J* = 9.4, 5.4 Hz, 2H), 2.22–2.15 (m, 2H), 2.08–2.01 (m, 1H), 1.98–1.87 (m, 1H), 1.65–1.57 (m, 2H),

1.44–1.25 (m, 8H). ¹³C NMR (126 MHz, DMSO-*d*₆) δ 174.1, 171.8, 171.6, 171.1, 171.0, 166.5, 161.0, 153.8, 151.0, 149.3, 148.8, 144.5, 129.2, 128.5, 128.2, 124.5, 123.7, 123.6, 123.4, 122.6, 121.7, 121.5, 121.4, 117.0, 111.5, 52.6, 46.2, 36.1, 32.3, 30.9, 29.4, 29.3, 29.0, 28.8, 26.9, 26.6, 25.4. HRMS (ESI) calcd for C₃₇H₄₃N₁₀O₆S [M+H]⁺ 755.3082 found 755.3075.

4.7.7.62. (*S*)-2-(4-(((2-Amino-4-oxo-3,4-dihydropteridin-6-yl)methyl)amino)benzamido)-5-((9-((2-amino-5-(thiophen-2-yl)phenyl)amino)-9-oxononyl)amino)-5-oxopentanoic acid (**24d**). Compound **23d** (0.034 g, 0.037 mmol) was dissolved in neat TFA (2 mL) and TIPS (0.5 mL) and stirred at room temperature for 2 h. The desired product **24d** (0.022 g, 79% yield) was obtained as described for the synthesis of **6**. ¹H NMR (500 MHz, DMSO-*d*₆) δ 8.67 (s, 1H), 7.66 (d, *J* = 8.4 Hz, 2H), 7.51 (s, 1H), 7.37 (d, *J* = 5.0 Hz, 1H), 7.28–7.21 (m, 2H), 7.08–7.02 (m, 1H), 6.80 (d, *J* = 8.3 Hz, 1H), 6.65 (d, *J* = 8.4 Hz, 2H), 4.51 (s, 2H), 4.35–4.25 (m, 1H), 3.05–2.97 (m, 2H), 2.34 (t, *J* = 7.3 Hz, 2H), 2.19 (t, *J* = 11.0 Hz, 2H), 2.11–2.00 (m, 1H), 1.97–1.86 (m, 1H), 1.67–1.54 (m, 2H), 1.40–1.22 (m, 10H). ¹³C NMR (126 MHz, DMSO-*d*₆) δ 174.1, 171.8, 171.6, 166.5, 161.0, 153.8, 151.0, 148.8, 144.4, 129.2, 128.5, 128.2, 123.7, 123.4, 122.6, 121.7, 121.5, 111.5, 52.6, 46.2, 36.1, 32.3, 29.4, 29.1, 29.0, 26.9, 26.7, 25.5. HRMS (ESI) calcd for C₃₈H₄₅N₁₀O₆S [M+H]⁺ 769.3239 found 769.3236.

Acknowledgments

We are grateful to Professor Olaf Wiest for providing us with the HDAC1 homology model. We thank Professor Philip S. Low for helpful discussion. This work was financially supported by NIH Grant R01CA131217 (A.K.O.) and R01GM084188 (MM) Q.H.S. is a recipient of a GAANN predoctoral fellowship from the Georgia Tech Center for Drug Design, Development, and Delivery and a dissertation fellowship from the Southern Regional Education Board (SREB).

Appendix A. Supplementary data

Supplementary data related to this article can be found at <http://dx.doi.org/10.1016/j.ejmech.2015.04.014>.

References

- [1] R.L. Strausberg, A.J.G. Simpson, L.J. Old, G.J. Riggins, Oncogenomics and the development of new cancer therapies, *Nature* 429 (2004) 469–474.
- [2] W.W. Ma, A.A. Adjei, Novel agents on the horizon for cancer therapy, *CA-Cancer J. Clin.* 59 (2009) 111–137.
- [3] B.E. Gryder, Q.H. Sodji, A.K. Oyeler, Targeted cancer therapy: giving histone deacetylase inhibitors all they need to succeed, *Future Med. Chem.* 4 (2012) 505–524.
- [4] L.M. Butler, X. Zhou, W.-S. Xu, H.I. Scher, R.A. Rifkind, P.A. Marks, V.M. Richon, The histone deacetylase inhibitor SAHA arrests cancer cell growth, up-regulates thioredoxin-binding protein-2, and down-regulates thioredoxin, *Proc. Natl. Acad. Sci.* 99 (2002) 11700–11705.
- [5] S. Minucci, P.G. Pelicci, Histone deacetylase inhibitors and the promise of epigenetic (and more) treatments for cancer, *Nat. Rev. Cancer* 6 (2006) 38–51.
- [6] M. Dokmanovic, C. Clarke, P.A. Marks, Histone deacetylase inhibitors: overview and perspectives, *Mol. Cancer Res.* 5 (2007) 981–989.
- [7] O. Witt, H.E. Deubzer, T. Milde, I. Oehme, HDAC family: what are the cancer relevant targets? *Cancer Lett.* 277 (2009) 8–21.
- [8] N. Ueki, S. Lee, N.S. Sampson, M.J. Hayman, Selective cancer targeting with prodrugs activated by histone deacetylases and a tumour-associated protease, *Nat. Commun.* 4 (2013) 2735.
- [9] W. Weichert, HDAC expression and clinical prognosis in human malignancies, *Cancer Lett.* 280 (2009) 168–176.
- [10] P. Porcu, H.K. Wong, We should have a dream: unlocking the workings of the genome in cutaneous T-cell lymphomas, *Clin. Lymphoma Myeloma Leuk.* 9 (2009) 409–411.
- [11] B.S. Mann, J.R. Johnson, M.H. Cohen, R. Justice, R. Pazdur, FDA approval summary: vorinostat for treatment of advanced primary cutaneous T-cell lymphoma, *Oncologist* 12 (2007) 1247–1252.

- [12] S. Subramanian, S.E. Bates, J.J. Wright, I. Espinoza-Delgado, R.L. Piekarz, Clinical Toxicities of Histone Deacetylase Inhibitors, Pharmaceuticals (Basel) 3, 2010, pp. 2751–2767.
- [13] J.S. de Bono, A. Ashworth, Translating cancer research into targeted therapeutics, *Nature* 467 (2010) 543–549.
- [14] T.Z. Qiu, L. Zhou, W. Zhu, T.S. Wang, J. Wang, Y.Q. Shu, P. Liu, Effects of treatment with histone deacetylase inhibitors in solid tumors: a review based on 30 clinical trials, *Future Oncol.* 9 (2013) 255–269.
- [15] A. Grassadonia, P. Cioffi, F. Simiele, L. Izzi, M. Zilli, C. Natoli, Role of hydroxamate-based histone deacetylase inhibitors (Hb-HDACs) in the treatment of solid malignancies, *Cancers* 5 (2013) 919–942.
- [16] J.A. Bauer, B.H. Morrison, R.W. Grane, B.S. Jacobs, S. Dabney, A.M. Gamero, K.A. Carnevale, D.J. Smith, J. Drazba, B. Seetharam, D.J. Lindner, Effects of interferon β on transcobalamin II-receptor expression and antitumor activity of Nitrosylcobalamin, *J. Natl. Cancer Instit.* 94 (2002) 1010–1019.
- [17] G. Russell-Jones, K. McTavish, J. McEwan, J. Rice, D. Nowotnik, Vitamin-mediated targeting as a potential mechanism to increase drug uptake by tumours, *J. Inorg. Biochem.* 98 (2004) 1625–1633.
- [18] L.T. Mantovani, S. Miotti, S. Ménard, S. Canevari, F. Raspagliesi, C. Bottini, F. Bottero, M.I. Colnaghi, Folate binding protein distribution in normal tissues and biological fluids from ovarian carcinoma patients as detected by the monoclonal antibodies MOv18 and MOv19, *Eur. J. Cancer* 30 (1994) 363–369.
- [19] N. Parker, M.J. Turk, E. Westrick, J.D. Lewis, P.S. Low, C.P. Leamon, Folate receptor expression in carcinomas and normal tissues determined by a quantitative radioligand binding assay, *Anal. Biochem.* 338 (2005) 284–293.
- [20] S.D. Weitman, R.H. Lark, L.R. Coney, D.W. Fort, V. Frasca, V.R. Zurawski, B.A. Kamen, Distribution of the folate receptor GP38 in Normal and malignant cell lines and tissues, *Cancer Res.* 52 (1992) 3396–3401.
- [21] W. Xia, P.S. Low, Folate-targeted therapies for cancer, *J. Med. Chem.* 53 (2010) 6811–6824.
- [22] Y. Lu, P.S. Low, Folate-mediated delivery of macromolecular anticancer therapeutic agents, *Adv. Drug Deliv. Rev.* 64 (Suppl.) (2012) 342–352.
- [23] P.S. Low, S.A. Kularatne, Folate-targeted therapeutic and imaging agents for cancer, *Curr. Opin. Chem. Biol.* 13 (2009) 256–262.
- [24] I.R. Vlahov, C.P. Leamon, Engineering folate–drug conjugates to target cancer: from chemistry to clinic, *Bioconjugate Chem.* 23 (2012) 1357–1369.
- [25] P.S. Low, W.A. Henne, D.D. Doorneweerd, Discovery and development of folic acid-based receptor targeting for imaging and therapy of cancer and inflammatory diseases, *Acc. Chem. Res.* 41 (2007) 120–129.
- [26] L. Matherly, Z. Hou, Y. Deng, Human reduced folate carrier: translation of basic biology to cancer etiology and therapy, *Cancer Metastasis Rev.* 26 (2007) 111–128.
- [27] C.P. Leamon, R.B. DePrince, R.W. Hendren, Folate-mediated drug delivery: effect of alternative conjugation chemistry, *J. Drug Target* 7 (1999) 157–169.
- [28] C.-Y. Ke, C.J. Mathias, M.A. Green, Targeting the tumor-associated folate receptor with an 111In–DTPA conjugate of pteric acid, *J. Am. Chem. Soc.* 127 (2005) 7421–7426.
- [29] A.K. Barton, A. Capdevila, Receptor-mediated folate accumulation is regulated by the cellular folate content, *Proc. Natl. Acad. Sci.* 83 (1986) 5983–5987.
- [30] J.C. Lundquist, Pelletier, Improved solid-phase peptide synthesis method utilizing α -azide-protected amino acids, *Org. Lett.* 3 (2001) 781–783.
- [31] S.-Y. Han, Y.-A. Kim, Recent development of peptide coupling reagents in organic synthesis, *Tetrahedron* 60 (2004) 2447–2467.
- [32] W. Lin, X. Zhang, Z. He, Y. Jin, L. Gong, A. Mi, Reduction of azides to amines or amides with zinc and ammonium chloride as reducing agent, *Synth. Commun.* 32 (2002) 3279–3284.
- [33] J. Luo, M.D. Smith, D.A. Lantrip, S. Wang, P.L. Fuchs, Efficient syntheses of pyrofolic acid and pteroyl azide, reagents for the production of carboxyl-differentiated derivatives of folic acid, *J. Am. Chem. Soc.* 119 (1997) 10004–10013.
- [34] A. Mehta, R. Jaouhari, T.J. Benson, K.T. Douglas, Improved efficiency and selectivity in peptide synthesis: use of triethylsilane as a carbocation scavenger in deprotection of t-butyl esters and t-butoxycarbonyl-protected sites, *Tetrahedron Lett.* 33 (1992) 5441–5444.
- [35] V. Patil, Q.H. Sodji, J.R. Kornacki, M. Mrksich, A.K. Oyelere, 3-Hydroxypyridin-2-thione as novel zinc binding group for selective histone deacetylase inhibition, *J. Med. Chem.* 56 (2013) 3492–3506.
- [36] Q.H. Sodji, V. Patil, J.R. Kornacki, M. Mrksich, A.K. Oyelere, Synthesis and structure–activity relationship of 3-hydroxypyridine-2-thione-based histone deacetylase inhibitors, *J. Med. Chem.* 56 (2013) 9969–9981.
- [37] B.E. Gryder, M.J. Akbashev, M.K. Rood, E.D. Raftery, W.M. Meyers, P. Dillard, S. Khan, A.K. Oyelere, Selectively targeting prostate cancer with antiandrogen equipped histone deacetylase inhibitors, *ACS Chem. Biol.* 8 (2013) 2550–2560.
- [38] K.J. Wallace, R. Hanes, E. Anslyn, J. Morey, K.V. Kilway, J. Siegel, Preparation of 1,3,5-tris(aminomethyl)-2,4,6-triethylbenzene from two versatile 1,3,5-tri(halosubstituted) 2,4,6-triethylbenzene derivatives, *Synthesis* 2005 (2005) 2080–2083.
- [39] S. Schäfer, L. Saunders, E. Eliseeva, A. Velena, M. Jung, A. Schwenhorst, A. Strasser, A. Dickmanns, R. Ficner, S. Schlimme, W. Sippl, E. Verdin, M. Jung, Phenylalanine-containing hydroxamic acids as selective inhibitors of class IIb histone deacetylases (HDACs), *Bioorg. Med. Chem.* 16 (2008) 2011–2033.
- [40] L. Santo, T. Hideshima, A.L. Kung, J.-C. Tseng, D. Tamang, M. Yang, M. Jarpe, J.H. van Duzer, R. Mazitschek, W.C. Ogier, D. Cirstea, S. Rodig, H. Eda, T. Scullen, M. Canavese, J. Bradner, K.C. Anderson, S.S. Jones, N. Raje, Pre-clinical activity, pharmacodynamic, and pharmacokinetic properties of a selective HDAC6 inhibitor, ACY-1215, in combination with bortezomib in multiple myeloma, *Blood* 119 (2012) 2579–2589.
- [41] J.L. Methot, P.K. Chakravarty, M. Chenard, J. Close, J.C. Cruz, W.K. Dahlberg, J. Fleming, C.L. Hamblett, J.E. Hamill, P. Harrington, A. Harsch, R. Heidebrecht, B. Hughes, J. Jung, C.M. Kenific, A.M. Kral, P.T. Meinke, R.E. Middleton, N. Ozerova, D.L. Sloman, M.G. Stanton, A.A. Szweczek, S. Tyagarajan, D.J. Witter, J. Paul Secrist, T.A. Miller, Exploration of the internal cavity of histone deacetylase (HDAC) with selective HDAC1/HDAC2 inhibitors (SHI-1: 2), *Bioorg. Med. Chem. Lett.* 18 (2008) 973–978.
- [42] P. Kumar, K. Lokanatha Rai, Reduction of aromatic nitro compounds to amines using zinc and aqueous chelating ethers: mild and efficient method for zinc activation, *Chem. Papers* 66 (2012) 772–778.
- [43] C.M. Paulos, J.A. Reddy, C.P. Leamon, M.J. Turk, P.S. Low, Ligand binding and kinetics of folate receptor recycling in vivo: impact on receptor-mediated drug delivery, *Mol. Pharmacol.* 66 (2004) 1406–1414.
- [44] H. Chen, R. Ahn, J. Van den Bossche, D.H. Thompson, T.V. O'Halloran, Folate-mediated intracellular drug delivery increases the anticancer efficacy of nanoparticle formulation of arsenic trioxide, *Mol. Cancer Ther.* 8 (2009) 1955–1963.
- [45] T. Suzuki, S. Hisakawa, Y. Itoh, N. Suzuki, K. Takahashi, M. Kawahata, K. Yamaguchi, H. Nakagawa, N. Miyata, Design, synthesis, and biological activity of folate receptor-targeted prodrugs of thiolate histone deacetylase inhibitors, *Bioorg. Med. Chem. Lett.* 17 (2007) 4208–4212.
- [46] G. Simmons, A.J. Rennekamp, N. Chai, L.H. Vandenbergh, J.L. Riley, P. Bates, Folate receptor alpha and caveolae are not required for Ebola virus glycoprotein-mediated viral infection, *J. Virol.* 77 (2003) 13433–13438.
- [47] J.A. Bergman, K. Woan, P. Perez-Villarreal, A. Villagra, E.M. Sotomayor, A.P. Kozikowski, Selective histone deacetylase 6 inhibitors bearing substituted urea linkers inhibit melanoma cell growth, *J. Med. Chem.* 55 (2012) 9891–9899.
- [48] S. Senese, K. Zaragoza, S. Minardi, I. Muradore, S. Ronzoni, A. Passafaro, L. Bernard, G.F. Draetta, M. Alcalay, C. Seiser, S. Chiocca, Role for histone deacetylase 1 in human tumor cell proliferation, *Mol. Cell. Biol.* 27 (2007) 4784–4795.
- [49] C. Chen, J. Ke, X.E. Zhou, W. Yi, J.S. Brunzelle, J. Li, E.-L. Yong, H.E. Xu, K. Melcher, Structural basis for molecular recognition of folic acid by folate receptors, *Nature* 500 (2013) 486–489.
- [50] M. Bantscheff, C. Hopf, M.M. Savitski, A. Dittmann, P. Grandi, A.-M. Michon, J. Schlegl, Y. Abraham, I. Becher, G. Bergamini, M. Boesche, M. Delling, B. Dumpelfeld, D. Eberhard, C. Huthmacher, T. Mathieson, D. PoECKel, V. Reader, K. Strunk, G. Sweetman, U. Kruse, G. Neubauer, N.G. Ramsden, G. Drewes, Chemoproteomics profiling of HDAC inhibitors reveals selective targeting of HDAC complexes, *Nat. Biotech.* 29 (2011) 255–265.
- [51] K.V. Butler, J. Kalin, C. Brochier, G. Vistoli, B. Langley, A.P. Kozikowski, Rational design and simple chemistry yield a Superior, neuroprotective HDAC6 inhibitor, Tubastatin A, *J. Am. Chem. Soc.* 132 (2010) 10842–10846.
- [52] R. Zhao, S.H. Min, Y. Wang, E. Campanella, P.S. Low, I.D. Goldman, A role for the proton-coupled folate transporter (PCFT-SLC46A1) in folate receptor-mediated endocytosis, *J. Biol. Chem.* 284 (2009) 4267–4274.
- [53] M.P. Carrasco, E.A. Enyedy, N.I. Krupenko, S.A. Krupenko, E. Nuti, T. Tuccinardi, S. Santamaria, A. Rossello, A. Martinelli, M. Amelia Santos, Novel folate-hydroxamate based antimetabolites: synthesis and biological evaluation, *Med. Chem.* 7 (2011) 265–274.
- [54] Z.A. Gurard-Levin, K.A. Kilian, J. Kim, K. Bähr, M. Mrksich, Peptide arrays identify isoform-selective substrates for profiling endogenous lysine deacetylase activity, *ACS Chem. Biol.* 5 (2010) 863–873.
- [55] Z.A. Gurard-Levin, M.D. Scholle, A.H. Eisenberg, M. Mrksich, High-throughput screening of small molecule libraries using SAMDI mass spectrometry, *ACS Comb. Sci.* 13 (2011) 347–350.
- [56] O. Trott, A.J. Olson, AutoDock Vina: Improving the speed and accuracy of docking with a new scoring function, efficient optimization, and multi-threading, *J. Comput. Chem.* 31 (2010) 455–461.
- [57] B.E. Gryder, M.K. Rood, K.A. Johnson, V. Patil, E.D. Raftery, L.-P.D. Yao, M. Rice, B. Azizi, D.F. Doyle, A.K. Oyelere, Histone deacetylase inhibitors equipped with estrogen receptor modulation activity, *J. Med. Chem.* 56 (2013) 5782–5796.
- [58] A.K. Oyelere, P.C. Chen, L.P. Yao, N. Boguslavsky, Heterogeneous diazo-transfer Reaction: a facile unmasking of azide groups on amine-functionalized insoluble supports for solid-phase synthesis, *J. Org. Chem.* 71 (2006) 9791–9796.